

Received October 31, 2019, accepted December 2, 2019, date of publication January 6, 2020, date of current version January 14, 2020.

Digital Object Identifier 10.1109/ACCESS.2020.2963997

# An Overview of Electromagnetic Band-Gap Integrated Wearable Antennas

ADEL Y. I. ASHYAP<sup>1</sup>, SAMSUL HAIMI BIN DAHLAN<sup>1</sup>, ZUHAIIRIAH ZAINAL ABIDIN<sup>1</sup>, (Member, IEEE), MUHAMMAD INAM ABBASI<sup>2</sup>, MUHAMMAD RAMLEE KAMARUDIN<sup>1</sup>, (Senior Member, IEEE), HUDA A. MAJID<sup>1</sup>, (Member, IEEE), MUHAMMAD HASHIM DAHRI<sup>1</sup>, MOHD HAIZAL JAMALUDDIN<sup>3</sup>, (Member, IEEE), AND AKRAM ALOMAINY<sup>4</sup>, (Senior Member, IEEE)

<sup>1</sup>Center for Applied Electromagnetic Systems Research (EM Center), Faculty of Electrical and Electronic Engineering, Universiti Tun Hussein Onn Malaysia, Batu Pahat 86400, Malaysia

<sup>2</sup>Faculty of Electrical and Electronic Engineering Technology, Universiti Teknikal Malaysia Melaka, Durian Tunggal 76100, Malaysia

<sup>3</sup>Wireless Communication Centre, Faculty of Electrical Engineering, Universiti Teknologi Malaysia, Johor Bahru 81310, Malaysia

<sup>4</sup>Antennas and Electromagnetics Research Group, School of Electronic Engineering and Computer Science, Queen Mary University of London, London E1 4NS, U.K.

Corresponding authors: Samsul Haimi Bin Dahlan (samsulh@uthm.edu.my) and Zuhairiah Zainal Abidin (zuhairia@uthm.edu.my)

This work was supported in part by the Research Management Center (RMC), Universiti Tun Hussein Onn Malaysia, under Grant E15501, and in part by the Ministry of Education Malaysia (MOE) through the Fundamental Research Grant Scheme (FRGS) under Grant Vot No. K186.

**ABSTRACT** The recent advancement in the wireless technology has led to the advent of wearable antennas. These antennas are utilized for Wireless Body Area Networks (WBANs) purposes such as health-care, military sportive activities and identification systems. Compared to conventional antennas, wearable antennas operate in an environment which is in highly near proximity to the curved human body. Therefore, the wearable /flexible antenna performance parameters, including reflection coefficient, bandwidth, directivity, gain, radiation characteristic, Specific Absorption Rate (SAR), and efficiency are anticipated to be influenced by the coupling and absorption by the human body tissues. In addition, an electromagnetic band-gap structure is introduced in the wearable /flexible antenna designs to enable and give a high degree of isolation from the human body which also decreases the SAR dramatically. This paper reviews the state-of-the-art wearable/flexible antennas integrated with the electromagnetic band-gap structure on flexible materials concentrating on single and dual-band designs. Besides, it also highlights the challenges and considerations for an appropriate wearable/flexible antenna.

**INDEX TERMS** Wearable/flexible antennas, EBG, AMC, metamaterials, metasurface, textile/fabric antennas, WBAN applications, ISM, SAR.

## I. INTRODUCTION

Wearable devices are critical in the ICT field for on-body applications and the deployment of the Internet of Things and Wireless Sensor Networks. They must be low-powered, small, and capable of connecting to a hub or gateway device to access the internet or the cloud. The goal of these devices is to enhance the quality of life by improving the functionality of clothing by combining fabrics and electronics. They are continually showing a vision of the future since they are

going to be an essential part of daily clothing and serve as an intelligent personal assistant [1]–[3].

With the tremendous growth of wearable devices, academics, engineers, and researchers are concentrating on the investigation of “Wireless Body Area Networks” (WBAN) that link different electronic devices on the human body. The WBANs have a variety of applications in our daily lives. In the healthcare arena, they are applied to monitor a patient’s serious health condition, such as a glucose monitoring system, capsule endoscopy, and blood pressure. Furthermore, they can be utilized in entertainment, military, business, and rescue operations, as well as incorporated into helmets, raincoats, shoes, jackets in emergency and rescue

The associate editor coordinating the review of this manuscript and approving it for publication was Chow-Yen-Desmond Sim<sup>1</sup>.

**TABLE 1. Wireless body area networks applications [10]–[12].**

Application	Description
Military/Space/Rescue	Battle field personnel care and intelligence, smart suits, fire detection, astronaut monitoring.
Entertainment	Wearable computing, Intelligent shoes, LED dresses, Wireless Digital, music jackets, smartwatches, Video Disc.
Healthcare/Medical	Treatment and drug delivery system, Wearable thermometer, wearable Doppler unit, sleep control, breast cancer detection, GPS tracker, patient monitoring, oximetry, endoscopy, smart diagnosis, glucose monitoring, aging care.
Business	Identification of individual peripheral devices, wireless transactions
Rescue and Security	Life jackets, rain coats, E-shoes, fitness bonds, trackers, helmets
Other	Aiding professional and amateur sport training, intelligent transportation systems, tourism, real-time streaming, security.

response systems. Table 1 provides a brief overview of these applications [4]–[7].

As a vital component in the WBAN system, wearable antenna is important for wireless communication with other devices on or off the human body [8], [9]. A wearable antenna is “an antenna that is specifically designed to function while being worn on body”. It can communicate with other antennas on the surface of the body or with an external antenna. It has a direct impact on the size, shape and performance of the system. The physical integration of antennas to devices is a major issue for the designers as they must deal with additional features like safety and regulation constraints [10]–[12]. Nowadays, the tendency is to integrate more and more wireless devices as near as possible to the human body which is, however, known to be very hostile to RF signal because of its absorbing properties.

One of the most challenging aspects of designing wearable antennas is avoiding as much as possible the negative effect of the interaction between the antenna and the dissipative biological tissue. The human body detunes the antenna and may absorb a large amount of the radiated power, thus reducing the gain and changing the radiation pattern. It is, therefore, necessary to isolate the antenna in order to preserve its radiation characteristic as much as possible and to prevent hazardous biological effects [13]–[16]. Furthermore, the wearable antenna performance should be maintained for various bending conditions, thus getting suiting the body curvature or body movement. Hence, a flexible/semi-flexible substrate that has deformation capability is required [17], [18].

More than a few kinds of designs such as inverted-F antennas, microstrip patch antenna, Magneto-electric dipole antennas, substrate integrated waveguide antennas, single patch antennas, CPW antenna, dipole or monopole antennas on planar reflectors, and cavity-backed antennas have been studied for their appropriateness as wearable antennas [19]–[36]. However, these configurations possessed some disadvantages such as narrow bandwidth, high SAR, large lateral size, low Front to Back Ratio (FBR) and high back radiation. To overcome these disadvantages, an isolating layer placed

between the human body and antenna will diminish the power absorbed by human body tissue [37].

The works reported in [38], [39] demonstrated that antennas with a big ground plane could provide a desire to reduce radiation backward, increase the stability of the wearable/flexible antenna, and isolate the human body from the electromagnetic (EM) radiation. Nevertheless, large ground planes resulted in the increase of the size and rigidity of the wearable antenna, which made the design uncomfortable to the user. This led to the need for new antennas that were more suitable for operation in the vicinity of humans.

To overcome these problems, few configurations of electromagnetic band-gap (EBG) positioned underneath the antenna were used to alleviate antenna-human interactions [1], [5], [13], [15], [40]–[62]. These results improved the antenna performance such as efficiency, gain, Front to Back Ratio (FBR) and decreased the back radiation towards the body as well as the SAR level.

In this paper, the previous comprehensive works are highlighted in order to show the usefulness of integrating EBG structures with the wearable antenna. Prior to this, the critical design issues in the wearable antenna will be highlighted. Then, the selection of non-conducting and conducting materials and their impact on the performance of the wearable antenna are discussed by providing several data of different materials. Thereafter, EBG are described in details in terms of classification, type, characteristics, and methodological design.

## II. CRITICAL DESIGN ISSUES IN WEARABLE ANTENNAS

Unlike antennas embedded in portable devices, wearable antennas are intended to work in a complicated body environment. The issues under that environment that might cause huge effects on antenna performance can be summarized from [38], [63] as the following:

- (i) “Human body” interactions with the antennas: The “human body” can have a strong reaction to the wave propagating around because of the electromagnetic properties of its complex tissues. This might cause a huge detuning of antenna resonance over a large frequency range. However, the radiation of the antenna towards the body can result in serious health problems for human beings.
- (ii) Vicinity of “human body”: Wearable antennas must be designed to work properly near the “human body”. Additionally, special concern should be given to the “Specific Absorption Rate” (SAR), which helps to quantify the power absorption problems needed to meet the standard to avoid harm to the “human body”. Hence, in the vicinity of the “human body”, various aspects should be taken into accounts such as the power absorbed in the “human body”, radiation characteristic of the antenna, and input-matching performance.
- (iii) Variations in dimensions: Some features of the wearable antenna, such as compression and stretching, are typical for fabrics that are susceptible to deformation/bending

and can affect the performance and features of the antenna structures. As a result, “it will not be easy to mass-produce an antenna through the same radiation features even using the same materials”

- (iv) Water absorption: Textile antennas made of fabric materials are exposed to risks under bad weather due to existing voids that can easily absorb moisture and water that can shift the resonant frequencies of an antenna.
- (v) Uneven body surface and movement: These elements may distort the antenna structure if the antenna is made out of fabric material.

As mentioned above, besides the general needs of antenna design, there are a few extra necessities for wearable antenna design that must be fulfilled in order for wearable applications, in terms of both physical size and radiation features in the closeness of the “human body”. These include:

- (i) Light weight and compact size in order to be comfortable to wear.
- (ii) Considerable stability and flexibility. The antenna is desirable to have a certain resistance to bending, and stretching.
- (iii) Capable of providing certain radiation shielding to the body. The international standard of Specific Absorption Rate must be satisfied for the purpose of safe communication on the body.

### III. MATERIAL CHARACTERIZATION FOR WEARABLE ANTENNA

Initially, it is essential to select a most suitable dielectric material for supporting layers (substrate) and conducting materials for radiating elements (patch, feeding line, ground plane). These dielectric and conducting materials are neatly selected to give a sensible amount of mechanical distortion with less impact of different weather conditions and suitable EM radiation protection. Thus, the wearable antenna will satisfy the property of comfort and safety to the users [63].

#### A. NON-CONDUCTING MATERIALS (SUBSTRATE)

The performance of constructed antennas relies on the substrate. This substrate not only offers a mechanical support, but it will impact on the antenna characteristics such as  $S_{11}$ , efficiency, and bandwidth [38], [63], [64]. Besides that, it is critical in terms of fabrication, operation, and wearability. The important characteristics that should be taken into consideration when selecting the substrate are permittivity, flexibility, thickness and loss tangent. The permittivity and thickness have an impact on the bandwidth, the flexibility enables the antenna to conform to the user, while the loss tangent has an impact on the efficiency. Thus, selecting a flexible substrate that is low in permittivity and loss tangent will increase the efficiency, especially in the presence of the human body. Therefore, a suitable substrate should satisfy both electrical and mechanical demands for the design [38], [63], [65].

TABLE 2. Summary of dielectric characteristics of textiles.

Materials	Permittivity	Loss tangent	Ref.
Fleece	1.17	0.0035	[13]
Silk	1.75	0.012	
PTFE	2.05	2.57	
Felt	1.38	0.023	
Panama	2.12	0.018	
Perspex	2.57	0.008	
Moleskin	1.45	0.05	
Tween	1.69	0.0084	
Silk	1.2	0.054	[63]
Cotton	1.54	0.058	
Felt	1.36	0.016	
Neoprene rubber	5.2	0.025	
Fleece	1.2	0.004	
Polyester foam	1.02	0.00009	
Leather	1.83-2.39	0.049-0.071	
different type			
Cordura/Lycra®	1.5	0.0093	[68]
Denim	1.4-2	0.014-0.07	
Cotton	1.6,1.54	0.04,0.058	
Polyester	1.9	0.0045	
Silk	1.75,1.2	0.012,0.054	
Moleskin	1.45	0.05	
Velcro	1.34	0.006	
Felt	1.36,1.38	0.016,0.023	
Tween	1.69	0.0084	
Fleece	1.17,1.2	0.0035,0.004	
Leather	1.8-2.95	0.049-0.16	
Panama	2.12	0.018	
Neoprene	5.2	0.03	
Denim	1.7, 1.7, 1.8	0.07, 0.085, 0.07	[1],[59],[69]
PDMS	2.67-3	0.01-0.05	[61],[70],[71]
PDMS	2.8,2.8	0.02,0.0013	[43],[72]

The properties of fabric/textile substrates vary with the selection of materials and frequencies. Therefore, a precise characterization of the properties of fabric substrates is essential before designing a fabric antenna [66], [67]. A summary of the characteristics that a number of researchers utilized for antenna designs is illustrated in Table 2.

The impacts of several flexible substrate parameters on the performance of an antenna were examined in [67], [73]. In conclusion, the flexible substrate provide acceptable gain, high efficiency, and stable radiation patterns without impacting bandwidth at deforming conditions.

To encapsulate, the selection of flexible materials are critical to the realization of a wearable antenna. Because of their conformality, flexible materials have become of great interest in replacing rigid substrates. These flexible materials can be wisely selected to resist distortion conditions such as twisting, stretching, crumpling, bending, and even distortion while retaining user comfort. In addition, wearable antennas essentially need a low loss dielectric material as their substrate, since great losses affect the antenna performance and efficiency.

#### B. CONDUCTING MATERIALS

As the fabric requires the conducting materials to serve as radiators, textile conducting materials are used to perform fully wearable/flexible antenna designs; therefore, it is deemed essential to characterize their electrical

TABLE 3. Summary of conducting material properties.

Conducting Material	Surface Resistivity, $\rho$ [ $\Omega\text{m}$ ]	Conductivity, $\sigma$ [S/m]	Thickness [mm]	Ref.
Shieldit Fabric	<0.05, <0.1	$1.18 \times 10^5$ , $6.67 \times 10^5$	0.17, 0.17	[45], [77], [78]
Taffeta Fabric	0.05	$2.5 \times 10^5$	0.08	[77], [78]
Copper Tape	-	$5.88 \times 10^7$ , $5.88 \times 10^7$	0.11, 0.03	[77], [79]
Zelt	0.01, -	$1 \times 10^6$ , $1.75 \times 10^5$	0.06, 0.0635	[13], [80]
AgNW/PDMS	-	$8.1 \times 10^5$	0.5	[81]
EgaIn liquid fillet	-	$2.5 \times 10^5$	0.08	[82]
PANI/CCo composite	-	$7.3 \times 10^3$	0.075	[83]
Polyleurethene-nanoparticle composite sheet	-	$1.1 \times 10^6$	0.0065	[84]

characteristics. Moreover, it is important to choose suitable conducting materials to ensure proper radiation characteristic of the antenna and keep the functionality of the clothes itself. Nevertheless, conductive material should meet a number of requirements such as:

- (i) Has a stable and low electrical resistance (1 ohm/square) to reduce losses.
- (ii) Essential to be homogeneous over the antenna area and the resistance variation across the materials must be small.
- (iii) Must be wearable/flexible so that the antenna cannot be distorted when worn.
- (iv) Must be inelastic because the electrical characteristics of elastic material may alter in the case of deforming, stretching, compression or curvature.

The conductivity characteristics of several materials utilized in the manufacture and packaging of the antenna play an essential role in attaining the required performances of antenna design. Several conducting materials are summarized in Table 3. The conductivity, ( $\sigma$ ), is calculated based on the value of the surface resistivity, ( $\rho_s$ ), and thickness of the textile material ( $t$ ) as in equation (1). Based on equation (1), the resistivity is inversely proportional to the conductivity, therefore as the resistivity is decreased, the conductivity increases, which diminishes the electrical losses and hence enhances antenna efficiency [13], [64], [74]–[76].

$$\sigma = \frac{1}{(\rho_s \cdot t)} \tag{1}$$

It can be concluded that the wearable antennas essentially desire low-loss dielectric materials as their substrate and highly conductive materials as conductors for efficient EM radiation reception/transmission.

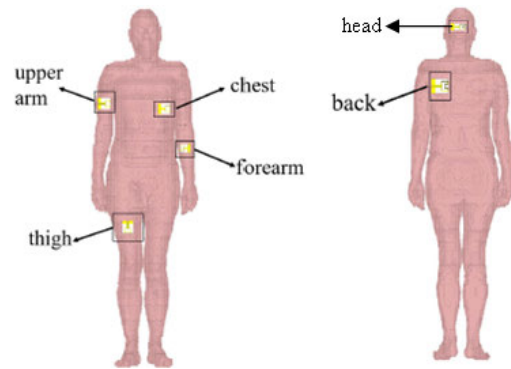


FIGURE 1. Human voxel model [47].

#### IV. HUMAN BODY BEHAVIOUR FOR WEARABLE ANTENNAS

The human body behaves as an irregular shaped medium. The body has conductivity dependent on frequency and “dielectric constant”. Therefore, in the wearable antenna design, it is essential to consider the interaction between the “human body” and the antenna. When the antenna moves closer to the “human body”, all common antenna parameters, including resonant frequency, radiation pattern, bandwidth, and especially efficiency, may change radically. Hence, the off-body (“free space”) design may simply be a rough assessment of the suitability of the antenna. To better comprehend these impacts, researchers/ academicians have introduced body models known as phantoms. These can be classified as Numerical Body Phantom (which utilizes simulated biological tissue) or as Physical Body Phantoms (which utilizes real physical structure) [39], [85]–[87].

The use of non-homogenous and complex phantom gives better results on the EM field measurements. Nevertheless, these phantoms require a lot of computational resources in the case of numerical simulation such as voxels models as shown in Fig.1. Therefore, it is better to produce a simple 3D model using only a part of the body in commercial simulation software.

Several models can be developed in the form of cylindrical, spherical and rectangular to represent, emulate and simulate the human arm, head, and chest or whole body, respectively. These numerical phantoms are desired in order to decrease the simulation time. These models can be modelled as multi-layer (non-homogenous) as shown in Fig. 2, or as a single layer (homogeneous). The multi-layer model consists of four layers in the form of cylindrical and rectangular phantoms, each layer representing bone (13 mm), muscle (20 mm), fat (5 mm) and skin (2 mm) [1]. On the other hand, spherical model consists of seven layers, each layer representing Brain (80 mm), CSF(Cerebro Spinal Fluid; 2 mm), Dura (1mm), Skull (10 mm), Muscle (4 mm), Fat (1 mm), and Skin (2 mm) [88]. The dielectric properties of the layers can be found in [1], [57], [88], [89], [89]–[91], [93].

A study was conducted in [94] using three different homogeneous models of the human body. The evaluation was based

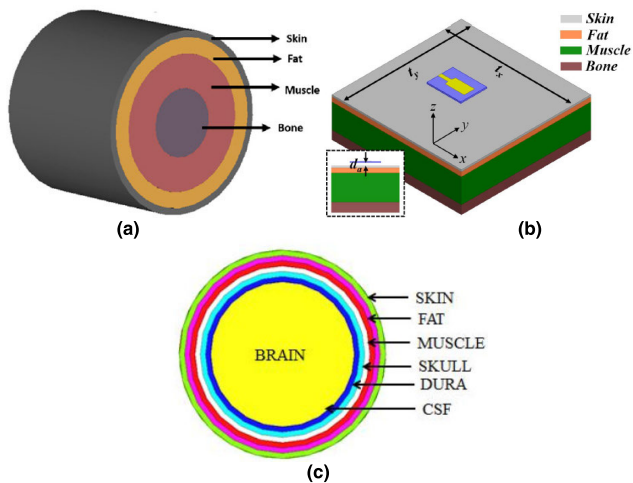


**FIGURE 2.** (a) The arm model [90] (b) The chest model [93] and (c) The head model [88].

on the accuracy, time consumption, computational efficiency, and resolution of the human body model results in software followed by experimental verifications. The phantoms were used to evaluate the performance of the antenna before loaded on a real body. Phantoms were also used to calculate the Specific Absorption Rate (SAR), which is known as the rate at which “RF electromagnetic energy is imparted to unit mass of biological body”. It was calculated using the formula given as equation (2): [49], [95].

$$SAR = \frac{\sigma |E|^2}{\rho} \quad (2)$$

where  $\sigma$  is “electrical conductivity”,  $E$  is “RMS electric field” and  $\rho$  is “sample density”.

General concern about the health impacts of radiation and legal requirements around the world has led researchers, academicians, and engineers to always be concerned about the amount of power absorbed by the “human body”. Therefore, SAR is an essential factor to compute the electromagnetic field absorbed by the “human body” in order to control the absorption of power below the level set by the standards [96], [97].

SAR is “typically averaged either over the whole body or over a small sample volume. It is directly proportional to the conductivity of the tissues absorbing the radiation and inversely proportional to its density” [68].

According to the guidelines given by the “International Commission on Non-Ionizing Radiation Protection” (ICNIRP) and “Federal Communications Commission” (FCC), the SAR levels must be less than 2 W/kg averaged over 10 g and less than 1.6 W/kg averaged over 1 g of “human body” tissues, respectively. Furthermore, the FCC standard from US (1.6 W/kg) is considered harder to satisfy than the ICNIRP from EU (2 W/kg), because of its lower limited value and smaller averaged mass with an average time of 6 min [98].

## V. ELECTROMAGNETIC BAND-GAP

The subject of the “Electromagnetic Band-Gap” (EBG) has become a rapidly growing topic for research among many academics, researchers and engineers around the world. These materials can offer distinct characteristics in controlling the propagation of electromagnetic waves. They can act like “perfect magnetic conductors” (PMC) that do not exist in nature. Thus, EBG is called an “artificial magnet connector” (AMC). They are defined as “artificial periodic (or sometimes non-periodic) objects that prevent/assist the propagation of electromagnetic waves in a specified band of frequency for all incident angles and all polarization states” [99]–[101].

EBG, also known as “photonic band-gap” (PBG), is a structure that is valuable in microwave application due to its periodic nature that prevents the propagation of certain electromagnetic wavelengths. The EBG material consists basically of periodically repeating high and low dielectric regions that create a band gap based on the periodicity of the structure. The EBG surface limits the propagation of surface waves within a particular frequency band (called a band gap), and thus decreases the level of undesired back lobe radiation towards the human body [99]–[101].

EBG materials are classified based on their arrangement into three-dimensional EBG structures (3-D), two-dimensional EBG structures (2-D), and one-dimension EBG structures (1-D). 3-D EBG is formed by stacking different EBG layers to form a three-dimensional structure such as a multi-layer metallic and tripod array. It exists in nature and is referred to as photonic band-gap materials. 2-D EBG is formed by arranging an EBG unit cell in two dimensions on a plane such as uni-planar design without vertical via and a mushroom-like structure. This type of EBG structure is preferable in antenna design. 1-D EBG is formed by arranging an EBG unit cell in one dimension to form a transmission line with two ports such as transmission line design [99], [102]–[104].

Although there are many different planar EBG configurations, the two main essential configurations are uniplanar electromagnetic band-gap (UC-EBG) and mushroom EBG. The UC-EBG is more popular and desired in wearable antennas due to its simplicity (no vias), low manufacturing cost and compatibility with standard planar circuit technology [38], [105].

To date, many UC-EBG structures have been introduced to increase the band-gap width and reduce the periodic size. For multi-band applications, multi-band EBGs have been introduced such as multi-layer EBG [106], [107], fractal EBG [56], [108], [109], and interdigitated unit [110]. On the other hand, it is preferable in wearable EBG to design simple structures because of the restriction of textile materials, as well as the difficulty of fabrication. Despite contentions [38] that mushrooms like EBGs cannot offer good performance compared to certain complex structures, its benefits such as ease of fabrication, low cost, and reliability still gain the most attention.



FIGURE 3. A wire current placed above PEC and EBG surface [38].

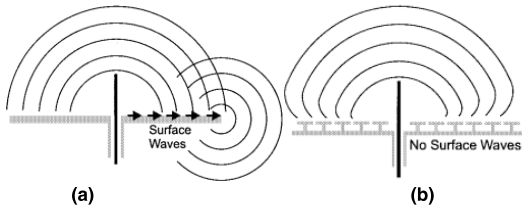


FIGURE 4. The effect of suppressing the surface waves (a) with surface wave, and (b) without surface wave [111].

According to [111], EBG has two interesting features over the frequency band known as band gap. First, its reflected wave is in phase with the incident wave. This property gives the EBG surface a function similar to PMC, which has a reflection phase of  $0^\circ$  but does not exist in nature. Second, it does not support the propagation of surface waves. These two features of EBG can solve some of the problems that occur in common antennas and optimize antenna performance; thus, it has an extensive range of applications in antenna design.

**A. IN-PHASE REFLECTION**

A simple wire antenna positioned on top of a PEC ground plane is depicted in Fig. 3. The image current below the perfect electric conducting ground plane is out of phase with the wire current. Meanwhile, in the presence of an EBG or PMC, the image current below the surface would be in phase with the wire current, thus improving the radiation of the antenna. EBG acts efficiently as an AMC that has a reflection phase of  $+1$  (in-phase reflection) in contrast to the traditional metal ground plane that has a reflection of  $-1$  (out of phase). Therefore, the EBG can act as a reflector that can reflect majority of the energy to the required direction.

**B. SUPPRESSING OF SURFACE WAVE**

Fig. 4 demonstrates another feature of the EBG surface. It can be utilized to eliminate the unwanted radiation caused by the finite ground planes. An “artificial impedance surface” which has certain band-gap features does not support propagation of the surface waves caused by the antenna.

Fig. 5(a) illustrates the radiation pattern of a monopole antenna on a metallic ground plane. The significant characteristics of the antenna pattern are the ripples are shown in the forward direction, and the amount of wasted power in the backward direction. Both of these characteristics are due to the surface wave that propagates away from the antenna and radiates from the ground level edges. If an EBG ground plane is used instead of the metal ground plane, as illustrated in Fig. 5(b), the surface wave is suppressed. It provides a

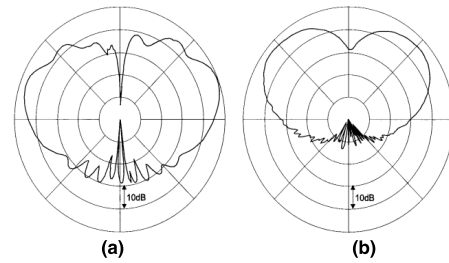


FIGURE 5. Measured radiation pattern of a vertical monopole antenna: (a) above PEC ground plane (PEC) and (b) above EBG ground plane [111].

smoother radiation pattern, with less wasted power in the backward hemisphere.

An EBG material in one form is a periodical structure in which high impedance exists for electromagnetic wave propagation within a certain frequency range. In antenna applications, the antenna can take advantage of the high impedance or surface wave band gap of an EBG within a particular frequency band. It has been found that antennas with EBG structures can offer remarkable improvements over conventional antennas [38].

For the purpose of wearable communication, EBG structure is desirable to decrease the backward radiation towards the “human body”, improve the radiation patterns in the forward direction, and therefore increases the gain and enhances “Front to Back Ratio” (FBR) of low-profile printed antennas. EBG also restricts the value of SAR to a safe level and improves the antenna performance and efficiency in the vicinity of the body. Hence, the incorporation of EBG into wearable/flexible systems has been of benefit in many ways [63], [112].

**C. OVERVIEW OF EBG PRINCIPLE**

EBG structures are typically periodical cells consisting of dielectric elements or metal. A mushroom-like EBG structure was first introduced by Sevenpiper [99], [113]. As illustrated in Fig. 6, the structure consists of a dielectric substrate, metal patches, ground plane, and connecting vias.

The operating mechanism of the EBG structure can be explained by an LC filter array or a parallel resonant circuit, as illustrated in Fig.7. The inductance is generated by a current loop within the structure through the pin vias, while the capacitance is generated by the gap of two adjacent patches. In the case of an EBG without vias, the inductance is due to the close proximity of the ground plane to the capacitive array of patches [38], [63].

The values of the capacitance ( $C$ ), inductance ( $L$ ), bandwidth ( $BW$ ) and resonant frequency ( $f_r$ ) are given by [111], [113]–[115]:

$$L = \mu_0 h \tag{3}$$

$$C = \frac{W \epsilon_0 (1 + \epsilon_r)}{\pi} \cosh^{-1} \left( \frac{W + g}{g} \right) \tag{4}$$

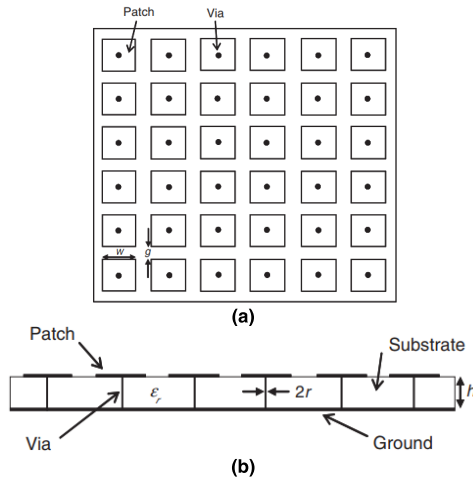


FIGURE 6. EBG surface: (a) front view and (b) cross-sectional view [113].

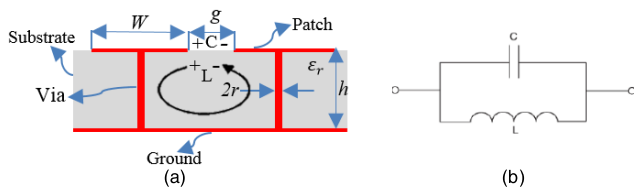


FIGURE 7. EBG unit-cell (a) vias EBG parameters and (b) lumped element equivalent circuit of the EBG [63].

$$f_r = \frac{1}{2\pi\sqrt{LC}} \quad (5)$$

$$BW = \frac{1}{\eta_0} \sqrt{\frac{L}{C}} \quad (6)$$

where  $\mu_0, \epsilon_0, \eta_0$ , are permeability, permittivity, and impedance of free space, respectively,  $g$  is the gap between adjacent patches and  $W$  is patch width.

At resonance, the surface impedance  $Z_s$  is determined by:

$$Z_s = \frac{j\omega L}{1 - \omega^2 LC} \quad (7)$$

Based on equations (3) to (7), the parameters that impacted the EBG design were investigated in [101], [116], [117]. They were substrate thickness, substrate permittivity, the gap between the unit cells and the patch width.

Examination of equation (7) revealed that at low frequencies, the unit cell is typically inductive and Transverse Magnetic (TM (red solid line)) surface wave was supported by this surface. As the frequency of excitation increased, the unit cells initially became resonant and then became capacitive with Transverse Electric (TE (blue dashed line)) wave becoming dominant mode. In a narrow band around the resonance frequency,  $\omega_0$  the surface showed high impedance. At resonance, the structure suppressed the propagation of the surface waves (TE and TM) and directed to the frequency band gap (EBG behavior) as revealed in Fig.8. Thus, the surface waves were suppressed and because of the high level of mismatch, a greater proportion of the energy in the system was reflected back. [63].

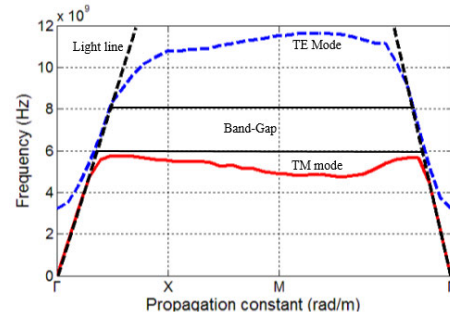


FIGURE 8. Dispersion diagram [118].

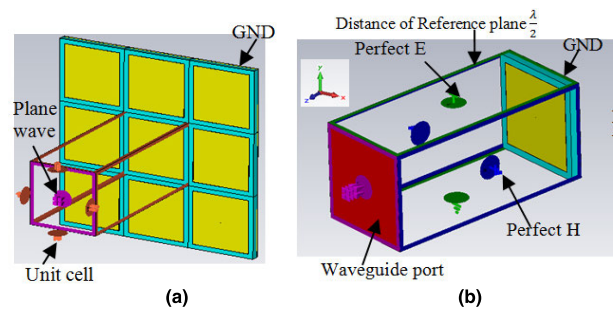


FIGURE 9. EBG unit cell model in CST microwave studio™ for reflection phase characterization based on (a) frequency domain and (b) time domain.

#### D. EBG CHARACTERIZATIONS

The features of EBG can be identified by reflection method, suspended line and desparation diagram as follows:

##### 1) REFLECTION PHASE CHARACTERISTIC OF EBG

The “reflection coefficient” is an essential parameter describing the reflection characteristics of an object. It is known as the ratio of the reflected field over the incident field at the reflective surface. Although the “PEC” and “PMC” surfaces present  $0^\circ$  and  $180^\circ$  reflection phases, respectively, to the incident wave, EBG offers a unique reflection phase ranging from  $180^\circ$  to  $-180^\circ$  [63], [99], [101], [119].

A unit cell model in “CST Microwave Studio™” using the frequency domain solver with two possible different boundary conditions was simulated to model an infinite and finite structure [24]. For infinite structure, the unit cell boundary conditions were imposed on the  $\pm y$  and  $\pm x$  directions. The plane wave was used for the excitation along  $+z$  while perfect electric ( $Et = 0$ ) was applied due to full ground along  $-z$  as shown in Fig. 9(a). In the case of finite structure, a perfect magnetic and electric conducting wall was imposed on  $\pm y$  and  $\pm x$  directions, respectively. The waveguide port was used to excite the signal along  $+z$  while perfect electric ( $Et = 0$ ) was applied due to full ground along  $-z$  as shown in Fig. 9(b). These boundary conditions were used to imitate the periodic nature of the used cell.

To obtain the reflection coefficient phase at the EBG surface, the plane wave or the waveguide ports must be de-embedded to the reflecting surface. The calculated reflection

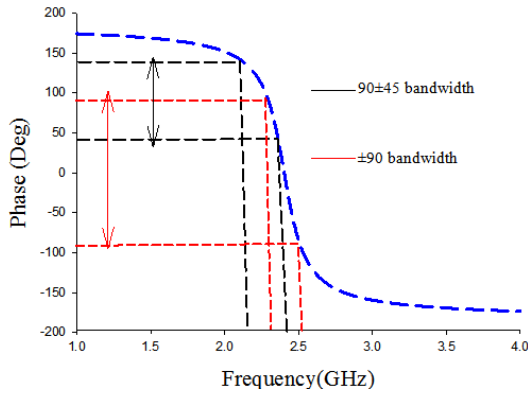


FIGURE 10. Reflection phase of EBG unit cell [2], [5].

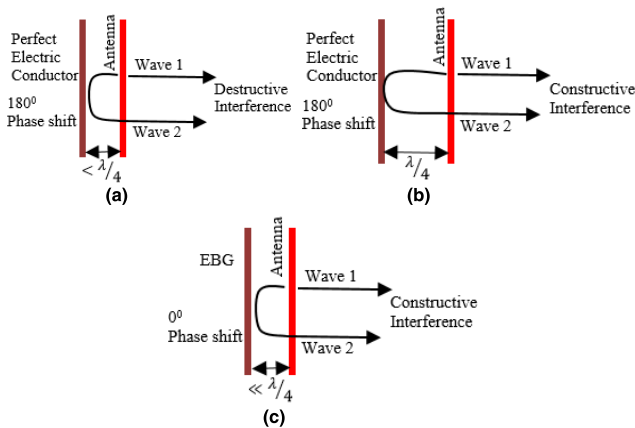


FIGURE 11. (a) Antenna placed close to metal ground. (b) Antenna placed far from the metal ground. (c) Antenna incorporated with EBG is in very close proximity with the ground layer [111].

coefficient phase of a general EBG structure was revealed in Fig. 10. The frequency ranges in which the reflection phase between  $90^\circ$  and  $-90^\circ$  had a surface impedance greater than the free space impedance. Nevertheless, it had been stated that the frequency ranges in which the reflection phase in the range of  $90^\circ \pm 45^\circ$  (as depicted in Fig. 10) attained a useful reflection coefficient of the low profile wire antenna [63], [99], [101], [119].

Reflection-phase is an important consideration because when an antenna that radiates in both directions was placed close to the EBG structure, the backward radiated EM energy can be reflected in phase with respect to forward radiated EM energy. This improves the total EM energy in the front half hemisphere of the antenna, which consequently raises the boresight gain of the antenna.

It is well known that when the radiating elements are placed in parallel and close to the conductive plane, it will suffer a significant reduction in radiation resistance because of opposing original current and the image current. Therefore, when the antenna was positioned near to the metal plate as revealed in Fig. 11(a), and the distance was less than a quarter wavelength,  $\lambda/4$ , the phase of the incoming wave was reversed upon reflection. This caused a destructive interference with

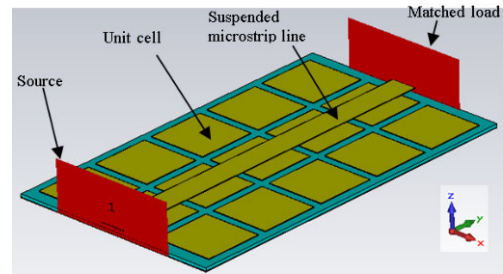


FIGURE 12. Method of suspended microstrip [2].

the wave propagating in another direction, and in addition, led to a poor radiation efficiency of antenna.

To solve this problem,  $\lambda/4$  was used between the radiating element and the ground plane, as revealed in Fig. 11(b). In this case, the antenna’s current and its image were in-phase and the wave add constructively. The antenna radiated efficiently, but the entire structure required a minimum thickness of  $\lambda/4$ .

In the case when EBG as a ground plane (which emulated a PMC in a specific frequency band) was introduced, the antenna could be placed much closer to the EBG as revealed in Fig. 11(c) due to its in-phase reflection features. As a result, all of the power was reflected in-phase, instead of destructively interfered, and the direction of the image current leads to constructive and led the antenna to radiate efficiently [38], [100], [111].

## 2) SUSPENDED LINE

A number of papers in [120]–[122] characterized EBG structure by utilizing an EBG array as a ground plane for a microstrip transmission line that was suspended over the array. This technique is similar to the implementation of EBG as a filter. The suspended microstrip line technique was utilized to determine the surface wave suppression features of the EBG structure. The technique was to insert the EBG between the microstrip and ground, forming a sandwich-like structure connecting with two  $50 \Omega$  SMA connectors placed at each edge as shown in Fig. 12. These SMA connectors were used to transmit and receive EM waves, thus the power transfer between them was computed. The band gap was usually considered at frequency range with attenuation losses of less than  $-10$  dB. The attenuation level relied on the number of unit-cell. As the number of the unit-cell was increased, the depth of the reduction band increased, so the power transfer reduction band was clearer.

## 3) DISPERSION DIAGRAM

Dispersion diagram is a “plot of the propagation constant versus frequency” [118]. It is a valuable tool to study the EBG at a desired frequency to show that the wave cannot propagate within the band-gap, hence the surface waves are suppressed. Frequently, the band-gap of a periodic structure is calculated from their dispersion characteristic, which is considered as an accurate representation of the surface wave property.

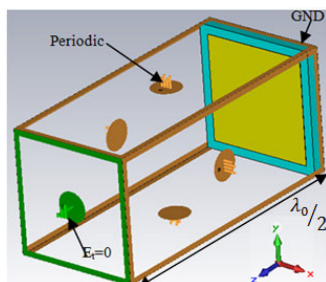


**FIGURE 13.** A unit cell model in CST microwave studio™ for band-gap characterization.

The study of band-gap was based on an infinite unit cell using the Eigenmode solver of “CST Microwave Studio™”. The unit cell of EBG structure under examination was drawn with periodic boundary condition (periodic walls are imposed on  $\pm x$  and  $\pm y$  directions of the unit cell while perfect electric ( $E_t = 0$ ) were imposed on  $\pm z$  directions) as shown in Fig 13. The phase shift was changed along the boundary of the irreducible Brillouin zone and the frequencies of Eigenmodes were achieved in each step. The steps were as follow:

- 1) The phase constant along the perpendicular direction  $y$  was fixed at 0 degrees. Correspondingly, “the phase constant along the  $x$ -direction, the base of the Brillouin triangle, called  $\Gamma - X$  direction, was varied from  $0^\circ$  to  $180^\circ$  degrees. Then, from numerical simulations or calculations of the dispersion equation, the first set of Eigenmode frequencies was found. This generated the frequency dataset for the wave propagation in the  $\Gamma - X$  segment of the Brillouin triangle.
- 2) The phase constant along the  $\Gamma - X$  segment of the Brillouin triangle  $x$ -direction was fixed at  $180^\circ$  degrees and the phase constant along the  $X - M$  segment,  $y$ -direction, was varied from  $0^\circ$  to  $180^\circ$  degrees. Then, from simulations or calculation of dispersion equation, the second set of Eigenmode frequencies was found.
- 3) The phase constant along with both segments,  $\Gamma - X$  and  $X - M$ , was varied in synchronization with each other from  $180^\circ$  to  $0^\circ$  degrees. Hence, the third set of Eigenmode frequencies was found for the  $M - \Gamma$  segment of the Brillouin triangle”.

Based on the above steps implemented in 3-D software such as CST Microwave Studio™, the dispersion diagram could be obtained as illustrated in Fig. 8 [118]. From Fig. 8, it is seen that the band gap existed between TM mode (solid line) and TE mode (dashed line) ranging from about 6 GHz to 8 GHz. It should be noted that the vias were responsible for these suppression band gaps. However, in the absence of vias, the stop band gaps disappeared, in other words, the band-gap shifted to a higher frequency [103].

## VI. IMPLEMENTATION OF EBG (VIALESS) IN WEARABLE APPLICATIONS

As stated in previous research [1], [5], [41], [45], [49], [57], [61], several papers were introduced for the design of

wearable antennas, but these designs suffered from several drawbacks that could limit the applications of wearable devices such as:

- Increase in SAR levels when working near body tissues, due to their nearly “bi-directional radiation” patterns.
- Protruded from the body and were therefore not low-profile or conformal.
- A significant amount of energy was directed into the “human body” because of their near- “Omni-directional radiation” properties.
- Exhibited a narrow bandwidth and poor FBR.
- Still retained a large lateral size.

In order to resolve these issues, EBG was introduced to be integrated with flexible antennas to offer a high degree of isolation between the “human body” and the antenna as well as reducing the SAR to the safety level.

The use of EBG structures in wearable antenna designs has been rapidly increased. In [55], the first proposed EBG based antenna design using a rigid substrate (FR-4) for wearable applications was presented. In spite of the fact that it was not a really wearable antenna as it was built of conventional inflexible FR4 substrate, the clue was still to utilize this for wearable applications. The antenna was printed on a thin FR4 substrate and the EBG pattern was etched on the ground plane of the antenna to operate at 2.45 GHz. It was noticed that the impact of EBG was to increase the bandwidth, diminish the size of the antenna, improve the gain and decrease the backward radiation.

The first invention of a fully wearable EBG antenna (WEBGA) using fabric materials was introduced in [40] with the extended version in [66]. The authors had discovered that integrating EBG with antenna could improve the bandwidth by 50% and reduce the antenna size by 30% from the original one. The authors also studied the impact of the bending of the wearable EBG on the input match. The antennas were bent around the cylinder along the principal  $x$ - $z$  and  $y$ - $z$  planes. It was observed that  $y$ - $z$  plane bending had a minor impact on the performance compared to  $x$ - $z$  plane bending. This was because  $x$ - $z$  plane bending altered the antennas resonant length. In addition, it was observed that the EBG antennas performed better than the traditional patch antennas.

The first in-depth investigations of textile EBG was done by Agneessens *et al.* [25]. They presented a dual-band coplanar antenna structure backed by  $3 \times 3$  arrays of textile EBG. The design was printed on a felt substrate. Reflection phase and suspended line methods were used to study the characteristics of the EBG. Based on the results, it was realized that using EBG for wearable application reduced the radiation into the body by over 10 dB, enhanced the antenna gain by 3 dB while achieving low back radiation and decreased SAR values by a factor of up to 20.

In addition, the researchers also investigated the bending effects on foam based on E-plane and H-plane configurations. Based on the results, the bandwidth remained the same at all times, but the bending in the E-plane affected the performance more than the H-plane. Furthermore, the integrated antenna

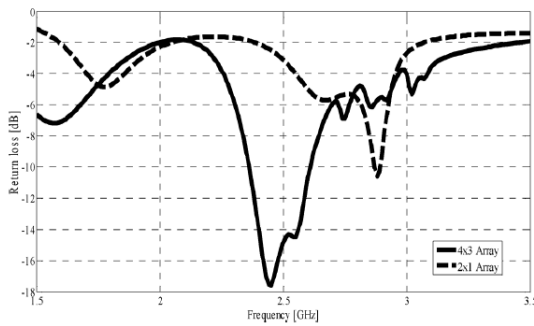


FIGURE 14. Investigation of increasing the unit cell number [15].

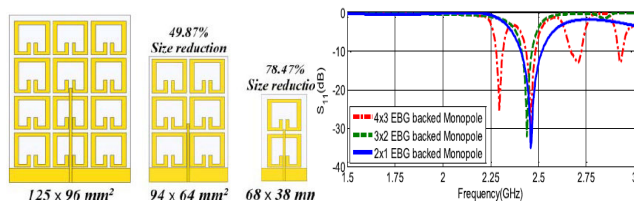


FIGURE 15. Variation of unit cell with S<sub>11</sub> at 2.45 GHz [46].

with EBG was placed directly on the body i.e. the thigh (jeans), the arm (skin), and on the back (cloth). It revealed that there were no significant changes between a measurement of foam and the human body. Nevertheless, at the higher frequency, the most shifting resonant frequency is on the human arm due to direct contact with the skin. In all cases, the bandwidth remained the same.

With the increasing success of integrated EBG with a wearable antenna in numerous applications, researchers started to explore a different type of flexible materials. In [15], a microstrip monopole antenna backed by an etched ground of  $4 \times 3$  arrays of single split-ring resonators as EBG was presented. The design was printed on paper as a substrate using inkjet-printed technology. The characteristic of EBG was studied based on the reflection phase. The study concentrated on the effect of the unit cell numbers, the size of the copper sheet and the placement of the antenna on the phantom. It was documented that as the number of unit cells and the copper sheet increased, a better result was achieved as illustrated in Fig. 14. Furthermore, the authors showed that when the antenna integrated with EBG was placed on a phantom, a better reflection coefficient was obtained compared to without EBG. In addition, adding EBG to the antenna showed an acceptable bandwidth of 4.08%.

In [46] a semi-flexible RT/Duroid 5880 substrate was used for the design of monopole antenna and EBG. The reflection phase method was used to determine the features of EBG. The authors reduced the number of unit cells from  $4 \times 3$  to  $2 \times 1$  EBG array while maintaining stable  $S_{11}$ . The variations of the unit cell number and the corresponding  $S_{11}$  of integrated design are shown in Fig 15. The final integrated design showed a good performance, such as the gain of 6.88 dBi, the bandwidth of 5% and SAR value of 0.244w/kg; even the size was compact. The design was loaded at several parts of

the human model tissue. The result revealed that a very stable  $S_{11}$  was sustained for all the cases even when the design was placed directly on the skin. This could be because the EBG had the feature of in-phase that can mimic the property of PMC which acted as isolation between the “human body” and the antenna. Hence, the incorporated antenna with EBG is suitable for “body-worn applications” where the antenna can be incorporated with a system for wearable biosensor or medical monitoring.

A Miniaturized slotted “Jerusalem Cross” (JC) “Artificial Magnetic Conductor” (EBG) integrated with the CPW M-shaped monopole antenna was presented for telemedicine applications at 2.45 GHz [49]. The antenna and EBG were fabricated on a different flexible substrate, Kapton polyimide with a “dielectric constant” of 3.5 and vinyl with a “dielectric constant” of 2.5, respectively. The EBG was analyzed based on the reflection phase method. The outcomes of the research show that the EBG contributed to increasing the gain by 3.7 dB, the “front to back ratio” of 8 dB and maintained 18% of the bandwidth. Furthermore, the antenna integrated with EBG eliminated the impedance mismatch and frequency shift caused by the “human body” tissues proximity compared to the antenna alone. In addition, the in-phase reflection feature of the EBG structures significantly decreased the unwanted electromagnetic radiation toward the patient’s body which was important for the performance of the telemedicine antenna system. Moreover, the SAR was studied to ensure the safety of the design for human health. Based on the numerical studies, the antenna alone had the SAR values of 1.88 W/Kg; adding EBG to the antenna has reduced the SAR level to 0.683W/Kg, which complied with the standard set by FCC. The SAR reduction achieved by adding EBG was 64%. The authors concluded that the integrated antenna with EBG would be “a good candidate for WBAN and telemedicine applications in terms of stability, bandwidth, SAR, and efficiency”.

According to [45] a dual-band (2.4 GHz and 5 GHz) textile antenna loaded with an “artificial magnetic conductor” (EBG) plane is proposed for WLAN applications. The antenna and EBG were printed on 1.5 mm felt substrate with the “dielectric constant” and loss tangent of 1.2 and 0.044, respectively. Shieldit™ Super conductive textile was used as conducting material with a thickness of 0.17 mm. The presented EBG helped to improve the FBR to higher than 12 dB in both bands while the realized gain of the antenna was about 2.5 dB at 2.45 GHz and between 0 to 4 dB in the higher band. Also, the antenna was placed on the arm and showed an acceptable reflection coefficient. The simulated bending was conducted along the x-axis and y-axis and for different radii. In the case of the x-axis, no significant changes were observed. This is because the direction of bending is parallel to the current on the patch and did not affect the current distribution considerably. In the case of the y-axis, the antenna changed more deeply as illustrated in Fig. 16. It was observed that at a lower band and as the radius is decreased, the resonant frequency shifted upwards but still covered the resonant

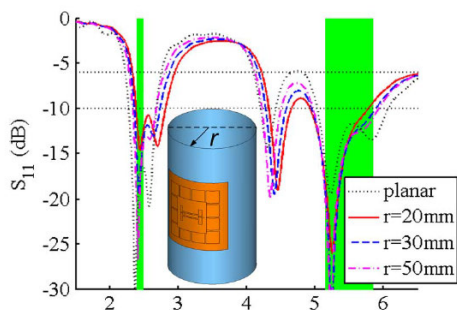


FIGURE 16. Simulated  $S_{11}$  of the integrated design based on bending [45].

TABLE 4. Performance comparison of the antenna with EBG with different ground size.

Frequency (GHz)	Antenna with 100×100 mm <sup>2</sup> ground (W/kg)	Antenna with 200×200 mm <sup>2</sup> ground (W/kg)
2.45	0.0464	0.00424
5.2	0.0232	0.00130
5.8	0.0300	0.00168

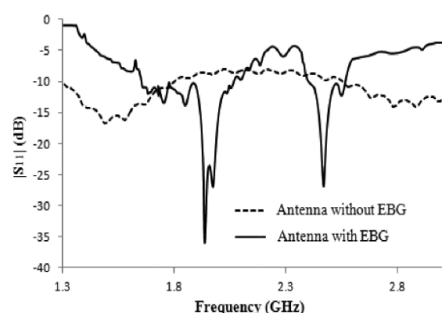


FIGURE 17.  $S_{11}$  characteristics of the antenna measured on body [56].

frequency at 2.45 GHz, while the upper band remained quasi unchanged where the only slight effect was seen at 5.85 GHz with  $S_{11}$  of  $-9.32$  dB. Moreover, the authors studied the effects of increasing the size of AMC on the SAR levels. The study was based on  $100 \times 100$  mm<sup>2</sup> and  $200 \times 200$  mm<sup>2</sup>, and the SAR results are summarized in Table 4. It is apparent that as the size is increased, the greater the reduction of SAR levels was achieved. The SAR values were reduced with a factor of more than 10.

A fractal geometry for wearable applications was presented in [56] for dual-band at GSM-1800 MHz and ISM-2.45 GHz band applications. The fractal-based antenna integrated with EBG structure was printed on 1 mm thick jeans fabric having a “dielectric constant” of 1.7 and a tangent loss of 0.085. The suspended technique was utilized to study the feature of EBG. The fractal-based monopole patch antenna was measured on “the human body” with and without EBG. Based on the results illustrated in Fig. 17, when the fractal-based monopole patch antenna was alone, the  $S_{11}$  was attenuated and detuned due to the high dielectric nature of the “human body” tissue, while when EBG was placed behind the antenna, the desired

TABLE 5. Comparison between monopole antenna with and without EBG and reference patch antenna.

	Monopole antenna	Reference patch antenna	Monopole antenna with EBG
$S_{11}$	$>-10$	$<-10$	$<-10$
BW (%)	0	2.9	5.5
Gain (dBi)	2	5.9	6.2
FBR (dB)	0	11	29
SAR (w/kg)	16.8	3.98	0.79

bands of operation were obtained. The bending and crumpling analysis are conducted. The result showed that the antenna with the EBG stills operates within the desired GSM and ISM bands without any appreciable frequency detuning. In addition, the EBG structure reduced the radiation into the “human body” by over 15 dB at both bands as well as the effect of frequency detuning due to the “human body”. Moreover, the SAR values of the antenna with EBG satisfied the safety limits compared to antenna alone.

A conformal wearable monopole antenna integrated with I-shaped EBG structure was introduced for “medical body-area network band” (MBAN) operating from 2.36 GHz to 2.4 GHz [57]. The I-shaped EBG unit cells were used to attain a high degree of isolation between the antenna and the human body. Compared to previous reported EBG, here the EBG behaved not only as a ground plane for isolation, but also as the main radiator. Without the integration of EBG, the monopole antenna demonstrated a poorly simulated and measured  $S_{11}$  while integrating with EBG improved the gain to 6.2 dBi, a bandwidth 5.5%, a “front-to-back ratio” higher than 23 dB and 95.3% reduction in the SAR. Further numerical and experimental studies showed that the performance of the antenna with EBG was extraordinarily robust to both structural bend and “human body” loading, far superior to both planar monopoles and microstrip patch antennas. A comparison between the monopole antenna, monopole antenna with EBG and reference patch antenna which had been commonly utilized for wearable applications was carried out to show the usefulness of integrated antenna with EBG as tabulated in Table 5.

Wearable antennas with linearly polarization (LP) could result in unreliable wireless links because of possible complete polarization mismatch as a result of the constant “human body” motion anticipated under realistic scenarios [61]. Therefore, circularly polarized (CP) antennas, in contrast, tend to be more favorable for wearable applications because of their enhanced signal robustness with respect to “human body” movement. Hence, a compact and flexible CP wearable antenna was presented for WBAN system for ISM band at 2.4 GHz. The design was based on PDMS as dielectric materials and silver nanowires (AgNWs) as conducting material. The anisotropic artificial ground plane behaved as EBG due to its in-phase feature. The proposed loop monopole antenna was placed over a truncating EBG of  $2 \times 2$ -unit cells to attain circularly polarized radiation. The proposed design revealed a good performance such as

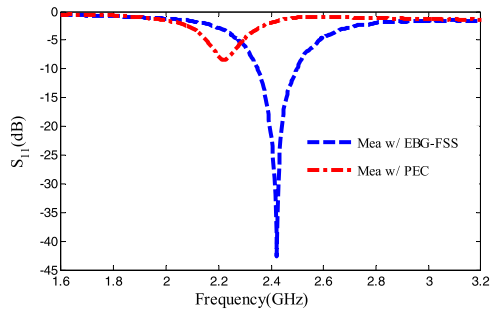


**FIGURE 18.** Experimental  $S_{11}$  of putting antenna above EBG-FSS and PEC as ground plane, respectively [1].

a gain of around 5.2 dBi, an axial ratio of less than 3 dB that covered the bandwidth of 69 MHz, FBR about 16 dB and a wide CP angular coverage in the targeted ISM band. Moreover, the proposed monopole antenna incorporated with EBG was compared with a conventional CP patch antenna of the same physical size, which was also comprised of the same PDMS and AgNW composite. The results showed that the presented monopole antenna incorporated with EBG had much more stable performance under deforming and “human body” loading, as well as a lower “specific absorption rate”. The simulated SAR was conducted using HUGO “human body” model in “CST Microwave Studio<sup>TM</sup>” for different parts at 2.44 GHz. The SAR of conventional CP patch antenna over 1 g averaged ranged from 0.22 to 0.29 W/kg, while for the presented integrated antenna with EBG for all three cases over 1 g averaged SAR varied from 0.13 to 0.18 W/kg. Thus, this showed that the maximum allowed accepted power for the proposed integrated antenna with EBG was about 65% higher than that for the CP patch antenna, thereby leading to a larger maximum communication distance of about 30%.

A wearable fabric CPW antenna based on an EBG-FSS was proposed for MBAN application at 2.4 GHz [1]. The design was printed on jeans substrate with “dielectric constant” of 1.7 and loss tangent of 0.07. The integration of EBG-FSS with CPW antenna revealed a good performance compared to the CPW antenna alone by improving the gain to 6.55 dBi, reducing SAR by 95%, enhancing the “front to back ratio” (FBR) by 13 dB and reducing the backward radiation towards the body. Furthermore, the authors demonstrated an experimental investigation of wearable periodic EBG-FSS structures and ordinary metal (PEC) to show the value of introducing of EBG-FSS in antenna designs. The proposed wearable CPW antenna was positioned over ordinary metal and EBG-FSS with the same substrate, dimensions, and height, to fairly compare. Based on the results that are revealed in Fig. 18, it is shown that when the antenna was placed over ordinary metal surface, a poor reflection coefficient was seen with  $S_{11} > -10$  at 2.4 GHz. As previously mentioned, this was because the ordinary metal surface had a phase of  $180^\circ$  which required at least a spacing of a  $\lambda/4$  to reflect in-phase. In this investigation, the spacing was less than  $\lambda/4$ , which caused an opposing direction of the current

of the wearable CPW antenna and the image current of the ordinary metal surface, resulting in a very poor  $S_{11}$ . Moreover, integrating the wearable CPW antenna with EBG-FSS demonstrated better  $S_{11} < -10$  at 2.4 GHz. This was because of the in-phase feature of EBG that reinforced the image current and the original current flow in the same direction. Hence, EBG appeared to be a good choice for a wearable low-profile antenna.

There is an increasing interest in research on wrist wear wireless communications and emerging technology has been deployed in a variety of applications such as smart-watches. The smart-watch wearable/flexible antennas have to be highly directive, low-profile, robust to the loading effect due to a “human body” and low specified absorption rate (SAR). EBG structures are particularly suitable to cope with these design goals. In order to enhance the communication quality of smart-watch applications, a low-profile antenna enabled by a miniaturized EBG was proposed to operate at 2.4 GHz [44]. The incorporated EBG with antenna resulted in a directivity of 6.3 dBi, and a bandwidth of 5.8%. Even though the incorporated antenna with EBG was situated in the close proximity to a “human body”, it still received more than 90% power, and the impedance matching is hardly influenced by the proximity loading of the components. In addition, the SAR value was studied and it was shown that with antenna alone, the SAR level was 13.5 W/kg, which exceeded the safety levels. On the other hand, integrating antenna with EBG reduced the SAR level to below the safety limit, which was 0.29 W/kg. Furthermore, the radiation efficiency was very robust against the loading effect due to wrist tissue. These features make the proposed EBG integrated with antenna a strong candidate for smart-watch applications.

“Radio Frequency Identification” (RFID) is a non-contact automatic identification technology. It consists of a number of a host computers, tags and a reader for managing information and service systems. RFID technologies have been broadly employed in our life and industry, such as education, medical, inventory, aviation, logistics, trade, transportation, and livestock [58], [62]. UHF RFID tags for smart clothing are always attached on the lossy medium objects. Nevertheless, tags antennas are susceptible to the impact of metal object or lossy media including a “human body” or water, though the RFID technologies have been utilized for many years. In order to solve the interference result by the lossy objects, an EBG was used to isolate the interference from the “human body” [58]. The EBG consisted of  $3 \times 3$ -unit cells underneath a circularly polarized cross-dipole tag antenna to attain longer read range for “UHF RFID” on-body application. The cross-dipole was applied on the phase-dependent EBG structure to accomplish high gain and isolate the impact of the “human body”. The designed was placed on the body to study its performances. The investigations revealed that the EBG increased the gain by 3.34 dB and assisted in producing CP wave. Furthermore, 3.2% measured impedance bandwidth was obtained which covered the “UHF RFID” bands of “North America and Taiwan”. The measurement revealed that the read range of

**TABLE 6.** Performance comparisons of tag with and without EBG on body.

Parameter	On the human model	
	Tag without EBG	Tag with EBG
Realized gain	-2.44 dBi	5.01 dBiC
Predicted reading range	5.34m	17.7m
Measured reading range	6m	15.7m
Radiation efficiency	13.1%	48%

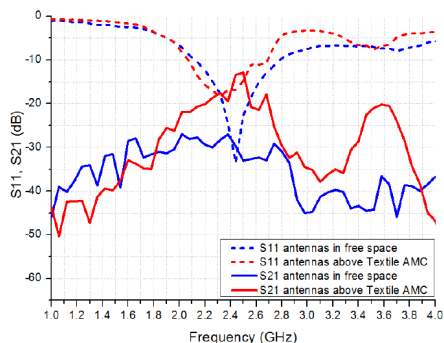


**FIGURE 19.** Measured S-parameters of antenna in several condition [59].

the tag pasted on a “human body” reached 15.7 meters when the reader had 4W EIRP, and the sensitivity of the microchip was -16.7 dBm. The usefulness of using EBG on the body in this study is shown in Table 6.

In addition, the investigations in [62] showed that with use of EBG, the metallic object/human tissue do not seriously degraded the behavior of the dipole antenna because of in-phase reflection characteristic of EBG that could insulate the user’s body from undesired exposure to electromagnetic radiation.

The propagation channels on the body are exposed to the effect of fading and shading. On-body channels are subjected to differences because of body movement, geometry of the body, and local scattering. On-body wearable antennas suffer from high propagation loss as well. Therefore, in all of these cases, the antennas attached to the human body were difficult to remain operational. To enable better wave propagation, EBG was utilized to improve transmissions from one antenna to another. In [59], two diamond dipole antennas were placed on top of waveguide jacket surfaces that consisted of EBG arrays. The dipole antennas had a fixed distance between them and each one was connected either to port 1 or port 2. Based on the result shown in Fig.19, the use of EBG contributes to improve the transmission between dipole antennas as recognized in  $S_{21}$  with a reduction of 16.3 dB. It showed that the electromagnetic coupling between the adjacent dipole antennas in the “body area network” correlated with wearable application could be improved by placing the antenna to the EBG waveguide, while attaining a better tolerance for matching the impedance of  $S_{11}$  and  $S_{22}$  from the connector to each of the individual antennas [53]. The improved coupling was because of the EBG capability to suppress the surface between the two dipole antennas. A number

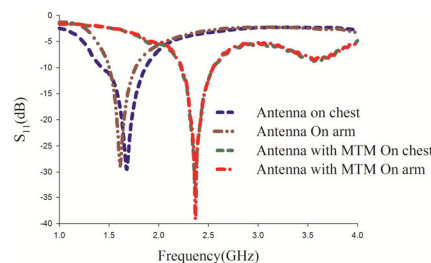


**FIGURE 20.**  $S_{11}$  behavior on the male volunteer with the antenna alone and with MTM [41].

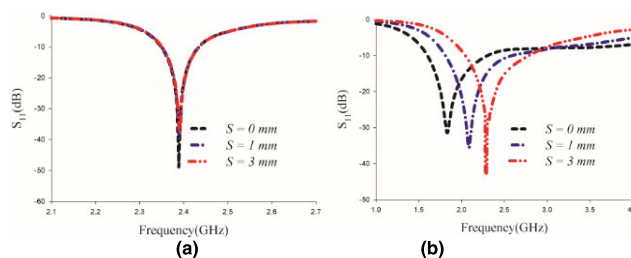


**FIGURE 21.**  $S_{11}$  behavior on model human chest with several distances.(a) MTM with antenna (a) U-shaped antenna alone [41].

of other researches on EBG for transmission enhancements between antennas have also been documented in [52], [53]. Transmitting between antennas are a vital factor, particularly in areas of body where multiple devices exist. Unlike free-space radiating antennas; antennas close to human body suffer significant losses and then degrade their performance. By employing EBG in the form of a wearable jacket beneath the antennas, efficient transmission between communication devices on-body environment can be further enhanced. EBG can behave as a reliable path for communication between two or more devices in “Wireless Body Area Network” (WBAN).

An investigation of the loading antenna alone and with MTM/EBG on body was carried out in [41]. Two parts of the body were chosen to evaluate the antenna alone and with MTM/EBG. Fig. 20 showed the result where it can be seen that when the antenna was alone, the  $S_{11}$  was detuned and attenuated due to dielectric properties of the body, whereas when the antenna was employed with MTM/EBG, the  $S_{11}$  is stable due to the MTM/EBG, which acted as isolation between the antenna and the body. Further investigations were conducted by placing the antenna with and without (w/o) MTM/EBG at several distances away from the body. The results are shown in Fig.21. It is seen that the  $S_{11}$  of the antenna alone was affected by the body compared to the antenna with MTM/EBG, which showed stable results. Furthermore, Fig. 21(b) shows that the  $S_{11}$  had shifted proportionally by the distance  $s$ , due to the high “dielectrics constant” of the “human body” tissues.

**VII. CONCLUSION**

This paper provides an overview of wearable antenna and their usefulness in several applications including health sector and military. It was found that with the growing success

TABLE 7. Comparison between antenna alone and antenna with EBG.

Ref	Antenna without EBG					Antenna with EBG				
	$S_{11}$ (on body)	Gain (dBi)	SAR (W/kg)	FBR (dB)		$S_{11}$ (on body)	Gain (dBi)	SAR (W/kg)	FBR (dB)	
				Off-body	On-body				Off-body	On-body
27	shifted	-	6.62	0	-	maintained as free space	-	0.016	15.6	18
28	shifted	1.74	5.41	0	13	maintained as free space	6.55	0.055	13	17
50	shifted	-4	16.8	0	16	maintained as free space	5.8	0.79	23	20
55	shifted	1.1	1.88	0	-	maintained as free space	4.7	0.6	8	-
70	shifted	2	7.78	0	-	maintained as free space	7.5	0.028	13.7	-
71	-	2.2	15	-	-	maintained as free space	6.3	0.29	-	-
72	shifted	2	6.19	0	-	maintained as free space	7.8	0.04	15.5	-

of wearable antenna designs, several flexible /textile substrates were investigated since the behaviors of the antennas depended on the features of the material. Therefore, it was deemed essential to characterize the performance of wearable antenna with several fabrics/flexible materials. The main consideration properties to determine fabric/flexible substrate are its permittivity and its loss tangent. Since the substrate is the crucial part of a wearable antenna, it should be designed by material that produces wide bandwidth and high efficiency. Furthermore, a substrate with low permittivity and thickness can help to reduce surface wave losses and as well improve the bandwidth. Hence, choosing an appropriate fabric/flexible material as substrate with the required radiation features is one of the main challenges in the fabrication of a good quality fabric/flexible antenna. The substrate thickness should be chosen such that the geometry of antenna remains compact and bandwidth of antenna improves. Nevertheless, the thickness may not optimize the efficiency. Hence, it is a tradeoff between bandwidth and efficiency of antenna in relation to its thickness. The performance of wearable antenna is anticipated to be affected by the coupling and absorption of the “human body” tissue. Therefore, “electromagnetic band gap” (EBG) structure is introduced to provide a high degree of isolation between the “human body” and the antenna. The EBG has two main interesting features, which is suppressing of surface wave and in-phase reflection rather than out of phase of plane waves. Hence, applying EBG for wearable antennas design helps to improve the directivity, the efficiency, the gain, FBR, the antenna’s radiation performance and reduce back radiation as well the “Specific Absorption Rate” (SAR). Based on the study on several applications of EBG in wearable applications and from the comparison that in Table 7 between antenna alone antenna with EBG, it can be concluded that by adding EBG structure, antenna becomes a strong potential candidate for wearable application, especially for medical applications.

## REFERENCES

- [1] A. Y. I. Ashyap, Z. Zainal Abidin, S. H. Dahlan, H. A. Majid, M. R. Kamarudin, A. Alomainy, R. A. Abd-Alhameed, J. S. Kosha, and J. M. Noras, “Highly efficient wearable CPW antenna enabled by EBG-FSS structure for medical body area network applications,” *IEEE Access*, vol. 6, pp. 77529–77541, 2018.
- [2] A. Y. Ashyap, S. H. Dahlan, Z. Z. Abidin, H. A. Majid, F. C. Seman, X. Ngu, and N. A. Cholan, “Flexible antenna with HIS based on PDMS substrate for WBAN applications,” in *Proc. IEEE Int. RF Microw. Conf. (RFM)*, Dec. 2018, pp. 69–72.
- [3] S. Genovesi, F. Costa, and G. Manara, “Compact antenna for wearable applications,” in *Proc. 2nd URSI Atlantic Radio Sci. Meeting (AT-RASC)*, May 2018, pp. 1–3.
- [4] A. Y. Ashyap, Z. Z. Abidin, S. H. Dahlan, H. A. Majid, M. R. Kamarudin, and R. A. Abd-Alhameed, “Robust low-profile electromagnetic band-gap-based on textile wearable antennas for medical application,” in *Proc. Int. Workshop Antenna Technol., Small Antennas, Innov. Struct., Appl. (iWAT)*, 2017, pp. 158–161.
- [5] A. Y. I. Ashyap, Z. Z. Abidin, S. H. Dahlan, H. A. Majid, S. M. Shah, M. R. Kamarudin, and A. Alomainy, “Compact and low-profile textile EBG-based antenna for wearable medical applications,” *IEEE Antennas Wireless Propag. Lett.*, vol. 16, pp. 2550–2553, 2017.
- [6] S. Seneviratne, “A survey of wearable devices and challenges,” *IEEE Commun. Surveys Tuts.*, vol. 19, no. 4, pp. 2573–2620, 4th Quart., 2017.
- [7] M. Chan, D. Estève, J.-Y. Fourniols, C. Escriba, and E. Campo, “Smart wearable systems: Current status and future challenges,” *Artif. Intell. Med.*, vol. 56, no. 3, pp. 137–156, Nov. 2012.
- [8] S. Yan, P. J. Soh, and G. Vandenbosch, “Made to be worn,” *Electron. Lett.*, vol. 50, no. 6, p. 420, Mar. 2014.
- [9] S. Yan, P. J. Soh, and G. A. E. Vandenbosch, “Wearable ultrawideband technology—A review of ultrawideband antennas, propagation channels, and applications in wireless body area networks,” *IEEE Access*, vol. 6, pp. 42177–42185, 2018.
- [10] A. Priya, A. Kumar, and B. Chauhan, “A review of textile and cloth fabric wearable antennas,” *Int. J. Comput. Appl.*, vol. 116, no. 17, pp. 1–5, Apr. 2015.
- [11] M. Seyedi, B. Kibret, D. T. H. Lai, and M. Faulkner, “A survey on intrabody communications for body area network applications,” *IEEE Trans. Biomed. Eng.*, vol. 60, no. 8, pp. 2067–2079, Aug. 2013.
- [12] Z. H. Jiang, M. D. Gregory, and D. H. Werner, “Design and experimental investigation of a compact circularly polarized integrated filtering antenna for wearable biotelemetric devices,” *IEEE Trans. Biomed. Circuits Syst.*, vol. 10, no. 2, pp. 328–338, Apr. 2016.
- [13] S. Zhu and R. Langley, “Dual-band wearable textile antenna on an EBG substrate,” *IEEE Trans. Antennas Propag.*, vol. 57, no. 4, pp. 926–935, Apr. 2009.

- [14] H. R. Raad, A. I. Abbosh, H. M. Al-Rizzo, and D. G. Rucker, "Flexible and compact AMC based antenna for telemedicine applications," *IEEE Trans. Antennas Propag.*, vol. 61, no. 2, pp. 524–531, Feb. 2013.
- [15] S. Kim, Y.-J. Ren, H. Lee, A. Rida, S. Nikolaou, and M. M. Tentzeris, "Monopole antenna with inkjet-printed EBG array on paper substrate for wearable applications," *IEEE Antennas Wireless Propag. Lett.*, vol. 11, pp. 663–666, 2012.
- [16] S. Genovesi, F. Costa, F. Fanciulli, and A. Monorchio, "Wearable inkjet-printed wideband antenna by using miniaturized AMC for sub-GHz applications," *IEEE Antennas Wireless Propag. Lett.*, vol. 15, pp. 1927–1930, 2016.
- [17] F. C. Seman, F. Ramadhan, N. S. Ishak, R. Yuwono, Z. Z. Abidin, S. H. Dahlan, S. M. Shah, and A. Y. I. Ashyap, "Performance evaluation of a star-shaped patch antenna on polyimide film under various bending conditions," *Prog. Electromagn. Res. Lett.*, vol. 85, pp. 125–130, Feb. 2019.
- [18] F. Seman, C. Manoharan, Z. Z. Abidin, and F. A. Poad, "Performance evaluation and implementation of semi-flexible dipole antenna for Internet of Things applications," in *Proc. IEEE Asia-Pacific Microw. Conf. (APMC)*, Nov. 2017, pp. 158–161.
- [19] H. Memarzadeh-Tehran, R. Abhari, and M. Niayesh, "A cavity-backed antenna loaded with complementary split ring resonators," *AEU-Int. J. Electron. Commun.*, vol. 70, no. 7, pp. 928–935, Jul. 2016.
- [20] P. Salonen, L. Sydanheimo, M. Keskilampi, and M. Kivikoski, "A small planar inverted-F antenna for wearable applications," in *Dig. Papers. 3rd Int. Symp. Wearable Comput.*, Jan. 2003, pp. 95–100.
- [21] A. Y. Ashyap, Z. Zainal Abidin, S. H. Dahlan, H. A. Majid, A. Waddah, M. R. Kamarudin, G. A. Oguntala, R. A. Abd-Alhameed, and J. M. Noras, "Inverted E-shaped wearable textile antenna for medical applications," *IEEE Access*, vol. 6, pp. 35214–35222, 2018.
- [22] H.-D. Chen, J.-S. Chen, and Y.-T. Cheng, "Modified inverted-L monopole antenna for 2.4/5 GHz dual-band operations," *Electron. Lett.*, vol. 39, no. 22, p. 1567, 2003.
- [23] H. Liu, P. Wen, S. Zhu, B. Ren, X. Guan, and H. Yu, "Quad-band CPW-fed monopole antenna based on flexible pentangle-loop radiator," *IEEE Antennas Wireless Propag. Lett.*, vol. 14, pp. 1373–1376, 2015.
- [24] S. Yan, P. J. Soh, and G. A. E. Vandenbosch, "Wearable dual-band magneto-electric dipole antenna for WBAN/WLAN applications," *IEEE Trans. Antennas Propag.*, vol. 63, no. 9, pp. 4165–4169, Sep. 2015.
- [25] R. Moro, S. Agneessens, M. Bozzi, and H. Rogier, "Wearable textile antenna in substrate integrated waveguide technology," *Electron. Lett.*, vol. 48, no. 16, pp. 985–987, Aug. 2012.
- [26] S. Agneessens, S. Lemey, T. Vervust, and H. Rogier, "Wearable, small, and robust: The circular quarter-mode textile antenna," *IEEE Antennas Wireless Propag. Lett.*, vol. 14, pp. 1482–1485, 2015.
- [27] A. Alomainy, Y. Hao, A. Owadally, C. G. Parini, Y. Nechayev, C. C. Constantinou, and P. S. Hall, "Statistical analysis and performance evaluation for on-body radio propagation with microstrip patch antennas," *IEEE Trans. Antennas Propag.*, vol. 55, no. 1, pp. 245–248, Jan. 2007.
- [28] M. N. Suma, P. C. Bybi, and P. Mohanan, "A wideband printed monopole antenna for 2.4-GHz WLAN applications," *Microw. Opt. Technol. Lett.*, vol. 48, no. 5, pp. 871–873, May 2006.
- [29] C.-H. Wu, T.-L. Li, M.-H. Hsieh, and J.-S. Sun, "An asymmetric shorted ground using CPW fed antenna for wearable device applications," in *Proc. IEEE Int. Conf. Consum. Electron.-Taiwan (ICCE-TW)*, Jun. 2017, pp. 95–96.
- [30] P. S. Hall, Y. Hao, Y. I. Nechayev, A. Alomainy, C. C. Constantinou, C. Parini, M. R. Kamarudin, T. Z. Salim, D. T. Hee, R. Dubrovka, A. S. Owadally, W. Song, A. Serra, P. Nepa, M. Gallo, and M. Bozzetti, "Antennas and propagation for on-body communication systems," *IEEE Antennas Propag. Mag.*, vol. 49, no. 3, pp. 41–58, Jun. 2007.
- [31] N. Haga, K. Saito, M. Takahashi, and K. Ito, "Characteristics of cavity slot antenna for body-area networks," *IEEE Trans. Antennas Propag.*, vol. 57, no. 4, pp. 837–843, Apr. 2009.
- [32] S. Agneessens and H. Rogier, "Compact half diamond dual-band textile HMSIW on-body antenna," *IEEE Trans. Antennas Propag.*, vol. 62, no. 5, pp. 2374–2381, May 2014.
- [33] Z. Muhammad, S. M. Shah, Z. Z. Abidin, A. Y. I. Ashyap, S. M. Mustam, and Y. Ma, "CPW-fed wearable antenna at 2.4 GHz ISM band," in *Proc. AIP Conf.*, vol. 1883, 2017, Art. no. 020003.
- [34] Q. Bai and R. Langley, "Crumpling of PIFA textile antenna," *IEEE Trans. Antennas Propag.*, vol. 60, no. 1, pp. 63–70, Jan. 2012.
- [35] P. J. Soh, G. A. E. Vandenbosch, S. L. Ooi, and N. H. M. Rais, "Design of a broadband all-textile slotted PIFA," *IEEE Trans. Antennas Propag.*, vol. 60, no. 1, pp. 379–384, Jan. 2012.
- [36] S. Yan, P. J. Soh, and G. A. E. Vandenbosch, "Dual-band textile MIMO antenna based on substrate-integrated waveguide (SIW) technology," *IEEE Trans. Antennas Propag.*, vol. 63, no. 11, pp. 4640–4647, Nov. 2015.
- [37] K. Chan, L. Fung, S. Leung, and Y. Siu, "Effect of internal patch antenna ground plane on SAR," in *Proc. 17th Int. Zurich Symp. Electromagn. Compat.*, 2006, pp. 513–516.
- [38] S. Zhu, "Wearable antennas for personal wireless," Ph.D. dissertation, Dept. Electron. Elect. Eng., Univ. Sheffield, Sheffield, U.K., 2008.
- [39] L. Ma, "On-body flexible printed antennas for body-centric wireless communications," Ph.D. dissertation, Dept. Elect. Eng., Loughborough Univ., Loughborough, U.K., 2010.
- [40] P. Salonen, F. Yang, Y. Rahmat-Samii, and M. Kivikoski, "WEBGA—Wearable electromagnetic band-gap antenna," in *Proc. IEEE Antennas Propag. Soc. Symp.*, vol. 1, Jun. 2004, pp. 451–454.
- [41] A. Y. I. Ashyap, Z. Zainal Abidin, S. H. Dahlan, H. A. Majid, and G. Saleh, "Metamaterial inspired fabric antenna for wearable applications," *Int. J. RF Microw. Comput. Aided Eng.*, vol. 29, no. 3, Mar. 2019, Art. no. e21640.
- [42] A. Y. Ashyap, W. N. N. W. Marzudi, Z. Z. Abidin, S. H. Dahlan, H. A. Majid, and M. R. Kamaruddin, "Antenna incorporated with electromagnetic bandgap (EBG) for wearable application at 2.4 GHz wireless bands," in *Proc. IEEE Asia-Pacific Conf. Appl. Electromagn. (APACE)*, Dec. 2016, pp. 217–221.
- [43] A. S. M. Alqadami, K. S. Bialkowski, A. T. Mobashsher, and A. M. Abbosh, "Wearable electromagnetic head imaging system using flexible wideband antenna array based on polymer technology for brain stroke diagnosis," *IEEE Trans. Biomed. Circuits Syst.*, vol. 13, no. 1, pp. 124–134, Feb. 2019.
- [44] Y.-S. Chen and T.-Y. Ku, "A low-profile wearable antenna using a miniature high impedance surface for smartwatch applications," *IEEE Antennas Wireless Propag. Lett.*, vol. 15, pp. 1144–1147, 2016.
- [45] S. Yan, P. J. Soh, and G. A. E. Vandenbosch, "Low-profile dual-band textile antenna with artificial magnetic conductor plane," *IEEE Trans. Antennas Propag.*, vol. 62, no. 12, pp. 6487–6490, Dec. 2014.
- [46] M. A. B. Abbasi, S. S. Nikolaou, M. A. Antoniadis, M. N. Stevanovic, and P. Vryonides, "Compact EBG-backed planar monopole for BAN wearable applications," *IEEE Trans. Antennas Propag.*, vol. 65, no. 2, pp. 453–463, Feb. 2017.
- [47] M. Wang, Z. Yang, J. Wu, J. Bao, J. Liu, L. Cai, T. Dang, H. Zheng, and E. Li, "Investigation of SAR reduction using flexible antenna with metamaterial structure in wireless body area network," *IEEE Trans. Antennas Propag.*, vol. 66, no. 6, pp. 3076–3086, Jun. 2018.
- [48] M. El Atrash, M. A. Abdalla, and H. M. Elhennawy, "A wearable dual-band low profile high gain low SAR antenna AMC-backed for WBAN applications," *IEEE Trans. Antennas Propag.*, vol. 67, no. 10, pp. 6378–6388, Oct. 2019.
- [49] H. R. Raad, A. I. Abbosh, H. M. Al-Rizzo, and D. G. Rucker, "Flexible and compact amc based antenna for telemedicine applications," *IEEE Trans. Antennas Propag.*, vol. 61, no. 2, pp. 524–531, Feb. 2013.
- [50] G.-P. Gao, C. Yang, B. Hu, R.-F. Zhang, and S.-F. Wang, "A wearable PIFA with an all-textile metasurface for 5 GHz WBAN applications," *IEEE Antennas Wireless Propag. Lett.*, vol. 18, no. 2, pp. 288–292, Feb. 2019.
- [51] A. Alemarayan and S. Noghian, "On-body low-profile textile antenna with artificial magnetic conductor," *IEEE Trans. Antennas Propag.*, vol. 67, no. 6, pp. 3649–3656, Jun. 2019.
- [52] K. Kamardin, M. K. A. Rahim, N. A. Samsuri, M. E. Jalil, I. H. Idris, and M. A. Abdul Majid, "Textile artificial magnetic conductor waveguide sheet with wire dipoles for body centric communication," *J. Teknol.*, vol. 64, no. 3, pp. 29–35, Oct. 2013.
- [53] K. Kamardin, M. K. A. Rahim, N. A. Samsuri, M. E. Jalil, and H. A. Majid, "Transmission enhancement using textile artificial magnetic conductor with coplanar waveguide monopole antenna," *Microw. Opt. Technol. Lett.*, vol. 57, no. 1, pp. 197–200, Jan. 2015.
- [54] P. Salonen and Y. Rahmat-Samii, "Textile antennas: Effects of antenna bending on input matching and impedance bandwidth," *IEEE Aerosp. Electron. Syst. Mag.*, vol. 22, no. 3, pp. 10–14, Mar. 2007.
- [55] P. Salonen, "A low-cost 2.45 GHz photonic band-gap patch antenna for wearable systems," in *Proc. 11th Int. Conf. Antennas Propag. (ICAP)*, no. 480, 2001, pp. 719–723.

- [56] S. Velan, E. F. Sundarsingh, M. Kanagasabai, A. K. Sarma, C. Raviteja, R. Sivasamy, and J. K. Pakkathillam, "Dual-band EBG integrated monopole antenna deploying fractal geometry for wearable applications," *IEEE Antennas Wireless Propag. Lett.*, vol. 14, pp. 249–252, 2015.
- [57] Z. H. Jiang, D. E. Brocker, P. E. Sieber, and D. H. Werner, "A compact, low-profile metasurface-enabled antenna for wearable medical body-area network devices," *IEEE Trans. Antennas Propag.*, vol. 62, no. 8, pp. 4021–4030, Aug. 2014.
- [58] J. H. Hong, C.-W. Chiu, and H.-C. Wang, "Design of circularly polarized tag antenna with artificial magnetic conductor for on-body applications," *Prog. Electromagn. Res. C*, vol. 81, no. 1, pp. 89–99, 2018.
- [59] K. Kamardin, M. K. Abd Rahim, N. A. Samsuri, M. E. B. Jalil, and I. H. Idris, "Textile artificial magnetic conductor waveguide jacket for on-body transmission enhancement," *Prog. Electromagn. Res. B*, vol. 54, pp. 45–68, Aug. 2013.
- [60] A. Y. Ashyap, Z. Z. Abidin, S. H. Dahlan, H. A. Majid, and F. C. Seman, "A compact wearable antenna using EBG for smart-watch applications," in *Proc. Asia-Pacific Microw. Conf. (APMC)*, Nov. 2018, pp. 1477–1479.
- [61] Z. H. Jiang, Z. Cui, T. Yue, Y. Zhu, and D. H. Werner, "Compact, highly efficient, and fully flexible circularly polarized antenna enabled by silver nanowires for wireless body-area networks," *IEEE Trans. Biomed. Circuits Syst.*, vol. 11, no. 4, pp. 920–932, Aug. 2017.
- [62] R. C. Hadarig, M. E. De Cos, and F. Las-Heras, "UHF dipole-AMC combination for RFID applications," *IEEE Antennas Wireless Propag. Lett.*, vol. 12, pp. 1041–1044, 2013.
- [63] S. Bashir, "Design and synthesis of non uniform high impedance surface based wearable antennas," Ph.D. dissertation, Dept. Elect. Eng., Loughborough Univ., Loughborough, U.K., 2009.
- [64] S. E. Florence, "Design development and performance evaluation of conformal textile antennas," Ph.D. dissertation, Dept. Commun. Eng., Anna Univ., Chennai, India, 2015.
- [65] Z. N. Chen, and M. Y. W. Chia, *Broadband Planar Antennas: Design and Applications*. Hoboken, NJ, USA: Wiley, 2006.
- [66] A. Tsolis, W. Whittow, A. Alexandridis, and J. Vardaxoglou, "Embroidery and related manufacturing techniques for wearable antennas: Challenges and opportunities," *Electronics*, vol. 3, no. 2, pp. 314–338, May 2014.
- [67] R. Salvado, C. Loss, R. Gonçalves, and P. Pinho, "Textile materials for the design of wearable antennas: A survey," *Sensors*, vol. 12, no. 11, pp. 15841–15857, Nov. 2012.
- [68] S. Zhang, "Design advances of embroidered fabric antennas," Ph.D. dissertation, Dept. Elect. Eng., Loughborough Univ., Loughborough, U.K., 2014.
- [69] B. Sanz-Izquierdo, J. Batchelor, and M. Sobhy, "Button antenna on textiles for wireless local area network on body applications," *IET Microw., Antennas Propag.*, vol. 4, no. 11, p. 1980, 2010.
- [70] G. J. Hayes, J.-H. So, A. Qusba, M. D. Dickey, and G. Lazzi, "Flexible liquid metal alloy (EGaIn) microstrip patch antenna," *IEEE Trans. Antennas Propag.*, vol. 60, no. 5, pp. 2151–2156, May 2012.
- [71] A. C. Myers, H. Huang, and Y. Zhu, "Wearable silver nanowire dry electrodes for electrophysiological sensing," *RSC Adv.*, vol. 5, no. 15, pp. 11627–11632, Jan. 2015.
- [72] J. Krupka, W. Gwarek, N. Kwietniewski, and J. G. Hartnett, "Measurements of planar metal-dielectric structures using split-post dielectric resonators," *IEEE Trans. Microw. Theory Techn.*, vol. 58, no. 12, pp. 3511–3518, Dec. 2010.
- [73] A. Rahman, M. T. Islam, M. J. Singh, and N. Misran, "Sol-gel synthesis of transition-metal doped ferrite compounds with potential flexible, dielectric and electromagnetic properties," *RSC Adv.*, vol. 6, no. 88, pp. 84562–84572, Aug. 2016.
- [74] I. Locher, M. Klemm, T. Kirstein, and G. Trster, "Design and characterization of purely textile patch antennas," *IEEE Trans. Adv. Packag.*, vol. 29, no. 4, pp. 777–788, Nov. 2006.
- [75] Y. Ouyang and W. Chappell, "High frequency properties of electrotextiles for wearable antenna applications," *IEEE Trans. Antennas Propag.*, vol. 56, no. 2, pp. 381–389, Feb. 2008.
- [76] M. K. Elbasheer, M. A. R. Osman, A. Abuelnuor, M. K. A. Rahim, and M. E. Ali, "Conducting materials effect on UWB wearable textile antenna," in *Proc. World Congr. Eng.*, in Lecture Notes in Engineering and Computer Science, vol. 1, 2014, pp. 372–376.
- [77] P. J. Soh, G. A. E. Vandenbosch, S. L. Ooi, and H. M. R. Nurul, "Characterization of a plain broadband textile PIFA," *Radioengineering*, vol. 20, no. 4, pp. 718–725, 2011.
- [78] M. Mantash, A.-C. Tarot, S. Collardey, and K. Mahdjoubi, "Investigation of flexible textile antennas and AMC reflectors," *Int. J. Antennas Propag.*, vol. 2012, pp. 1–10, 2012.
- [79] P. J. Soh, G. A. E. Vandenbosch, F. H. Wee, M. Zoinol, A. Abdul, and P. Campus, "Bending investigation of broadband wearable all-textile antennas," *Austral. J. Basic Appl. Sci.*, vol. 7, no. 5, pp. 91–94, 2013.
- [80] H. M. R. Nurul, F. Malek, P. J. Soh, and G. A. E. Vandenbosch, "Dual-band bench feed textile antenna," in *Proc. Int. Symp. Antennas Propag.*, 2010, pp. 709–712.
- [81] L. Song, A. C. Myers, J. J. Adams, and Y. Zhu, "Stretchable and reversibly deformable radio frequency antennas based on silver nanowires," *ACS Appl. Mater. Interfaces*, vol. 6, no. 6, pp. 4248–4253, Mar. 2014.
- [82] J.-H. So, J. Thelen, A. Qusba, G. J. Hayes, G. Lazzi, and M. D. Dickey, "Reversibly deformable and mechanically tunable fluidic antennas," *Adv. Funct. Mater.*, vol. 19, no. 22, pp. 3632–3637, Nov. 2009.
- [83] Z. Hamouda, J.-L. Wojkiewicz, A. A. Pud, L. Kone, S. Bergheul, and T. Lasri, "Magnetodielectric nanocomposite polymer-based dual-band flexible antenna for wearable applications," *IEEE Trans. Antennas Propag.*, vol. 66, no. 7, pp. 3271–3277, Jul. 2018.
- [84] Y. Kim, J. Zhu, B. Yeom, M. Di Prima, X. Su, J.-G. Kim, S. J. Yoo, C. Uher, and N. A. Kotov, "Stretchable nanoparticle conductors with self-organized conductive pathways," *Nature*, vol. 500, no. 7460, pp. 59–63, Aug. 2013.
- [85] K. Ito, C.-H. Lin, and H.-Y. Lin, "Evaluation of Wearable and Implantable Antennas with Human Phantoms," in *Handbook of Antenna Technologies*, vols. 1–4, Z. N. Chen, D. Liu, H. Nakano, X. Qing, and T. Zwick, Eds. Singapore: Springer, 2016, pp. 2239–2268.
- [86] I. Khan, "Diversity and MIMO for body-centric wireless communication channels," Ph.D. dissertation, Dept. Elect. Comput. Eng., Univ. Birmingham, Birmingham, U.K., 2009.
- [87] R. A. Valenzuela, "Antennas and propagation for body-centric wireless communications," in *Proc. Veh. Technol. Conf. (VTC)*, vol. 1, 2002, pp. 1–5.
- [88] L. Belrhiti, F. Riouch, A. Tribak, J. Terhzaz, and A. M. Sanchez, "Flexible antennas design and test for human body applications scenarios," *J. Microw., Optoelectron. Electromagn. Appl.*, vol. 16, no. 2, pp. 494–513, Apr. 2017.
- [89] V. Kumar and B. Gupta, "Swastika slot UWB antenna for body-worn application in WBAN," in *Proc. 8th Int. Symp. Med. Inf. Commun. Technol. (ISMICT)*, Apr. 2014, pp. 1–5.
- [90] M. Ullah, M. Islam, T. Alam, and F. Ashraf, "Paper-based flexible antenna for wearable telemedicine applications at 2.4 GHz ISM band," *Sensors*, vol. 18, no. 12, p. 4214, Dec. 2018.
- [91] S. Can and A. E. Yilmaz, "Reduction of specific absorption rate with artificial magnetic conductors," *Int. J. RF Microw. Comput. Aided Eng.*, vol. 26, no. 4, pp. 349–354, May 2016.
- [92] C. Gabriel, "Compilation of the dielectric properties of body tissues at RF and microwave frequencies," Brooks Air Force Base, San Antonio, TX, USA, Tech. Rep. AL/OE-RE-1996-0037, 1996.
- [93] Z. H. Jiang and D. H. Werner, "Robust low-profile metasurface-enabled wearable antennas for off-body communications," in *Proc. 8th Eur. Conf. Antennas Propag. (EuCAP)*, Apr. 2014, pp. 21–24.
- [94] M. Ur-Rehman, Q. H. Abbasi, X. Chen, and Z. Ying, "Numerical modelling of human body for Bluetooth body-worn applications," *Prog. Electromagn. Res.*, vol. 143, pp. 623–639, Aug. 2013.
- [95] *IEEE Recommended Practice for Measurements and Computations of Radio Frequency Electromagnetic Fields With Respect to Human Exposure to Such Fields, 100 kHz-300 GHz*, IEEE Standard C95.3-2002, (Revision of IEEE Standard C95.3-1991), 2002, p. i-126.
- [96] W. Whittow, C. Panagamuwa, R. Edwards, and J. Vardaxoglou, "The energy absorbed in the human head due to ring-type jewelry and face-illuminating mobile phones using a dipole and a realistic source," *IEEE Trans. Antennas Propag.*, vol. 56, no. 12, pp. 3812–3817, Dec. 2008.
- [97] W. Whittow and R. Edwards, "A study of changes to specific absorption rates in the human eye close to perfectly conducting spectacles within the radio frequency range 1.5 to 3.0 GHz," *IEEE Trans. Antennas Propag.*, vol. 52, no. 12, pp. 3207–3212, Dec. 2004.
- [98] K. Zhao, S. Zhang, Z. Ying, T. Bolin, and S. He, "SAR study of different MIMO antenna designs for LTE application in smart mobile handsets," *IEEE Trans. Antennas Propag.*, vol. 61, no. 6, pp. 3270–3279, Jun. 2013.

[99] D. Sievenpiper, L. Zhang, R. Broas, N. Alexopolous, and E. Yablonovitch, "High-impedance electromagnetic surfaces with a forbidden frequency band," *IEEE Trans. Microw. Theory Techn.*, vol. 47, no. 11, pp. 2059–2074, 1999.

[100] Y. Rahmat-Samii and F. Yang, *Electromagnetic Band Gap Structures in Antenna Engineering*. New York, NY, USA: Cambridge Univ. Press, 2009.

[101] F. Yang and Y. Rahmat-Samii, "Reflection phase characterizations of the EBG ground plane for low profile wire antenna applications," *IEEE Trans. Antennas Propag.*, vol. 51, no. 10, pp. 2691–2703, Oct. 2003.

[102] A. Barlevy and Y. Rahmat-Samii, "Characterization of electromagnetic band-gaps composed of multiple periodic tripods with interconnecting vias: Concept, analysis, and design," *IEEE Trans. Antennas Propag.*, vol. 49, no. 3, pp. 343–353, Mar. 2001.

[103] F.-R. Yang, K.-P. Ma, Y. Qian, and T. Itoh, "A uniplanar compact photonic-bandgap (UC-PBG) structure and its applications for microwave circuit," *IEEE Trans. Microw. Theory Techn.*, vol. 47, no. 8, pp. 1509–1514, 1999.

[104] V. Radisic, Y. Qian, R. Coccioli, and T. Itoh, "Novel 2-D photonic bandgap structure for microstrip lines," *IEEE Microw. Guided Wave Lett.*, vol. 8, no. 2, pp. 69–71, 1998.

[105] G. Goussetis, A. Feresidis, and J. Vardaxoglou, "Tailoring the AMC and EBG characteristics of periodic metallic arrays printed on grounded dielectric substrate," *IEEE Trans. Antennas Propag.*, vol. 54, no. 1, pp. 82–89, Jan. 2006.

[106] G. Goussetis, A. Feresidis, and J. Vardaxoglou, "FSS printed on grounded dielectric substrates: Resonance phenomena, AMC and EBG characteristics," in *Proc. IEEE Antennas Propag. Soc. Int. Symp.*, vol. 1B, Dec. 2005, pp. 644–647.

[107] A. Monorchio, G. Manara, and L. Lanuzza, "Synthesis of artificial magnetic conductors by using multilayered frequency selective surfaces," *IEEE Antennas Wireless Propag. Lett.*, vol. 1, pp. 196–199, 2002.

[108] F. Frezza, L. Pajewski, and G. Schettini, "Fractal two-dimensional electromagnetic bandgap structures," *IEEE Trans. Microw. Theory Techn.*, vol. 52, no. 1, pp. 220–227, Jan. 2004.

[109] E. Wang and Q. Liu, "GPS patch antenna loaded with fractal EBG structure using organic magnetic substrate," *PIER Lett.*, vol. 58, pp. 23–28, Dec. 2015.

[110] S. Rogers, W. Mckinzie, and G. Mendolia, "AMCs comprised of interdigital capacitor FSS layers enable lower cost applications," in *IEEE Antennas Propag. Soc. Int. Symp. Dig. USNC/CNC/URSI North Amer. Radio Sci. Meeting*, Mar. 2004, pp. 411–414.

[111] D. Sievenpiper, "High-impedance electromagnetic surfaces," Ph.D. dissertation, Dept. Elect. Eng., Univ. California, Los Angeles, Los Angeles, CA, USA, 1999.

[112] U. Ali, S. Ullah, J. Khan, M. Shafi, B. Kamal, A. Basir, J. A. Flint, and R. D. Seager, "Design and SAR analysis of wearable antenna on various parts of human body, using conventional and artificial ground planes," *J. Elect. Eng. Technol.*, vol. 12, no. 1, pp. 317–328, Jan. 2017.

[113] S. Rea, D. Linton, E. Orr, and J. Mcconnell, "Broadband high-impedance surface design for aircraft HIRF protection," *IEE Proc., Microw., Antennas Propag.*, vol. 153, no. 4, p. 307, 2006.

[114] G. Niyomjan and Y. Huang, "A suspended microstrip fed slot antenna on high impedance surface structure," in *Proc. 1st Eur. Conf. Antennas Propag.*, Nov. 2006, pp. 1–4.

[115] D. Ramaccia, A. Toscano, and F. Bilotti, "A new accurate model of high-impedance surfaces consisting of circular patches," *Prog. Electromagn. Res. M*, vol. 21, pp. 1–17, May 2011.

[116] Z. Wei, C. Guo, J. Ding, N. Li, and Z. Wei, "Parametric analysis of the EBG structure and its application for low profile wire antennas," in *Proc. 8th Int. Symp. Antennas, Propag. EM Theory*, Nov. 2008, pp. 561–564.

[117] H. M. El-Maghrabi, A. M. Attiya, E. A. Hashish, and H. S. Sedeeq, "Parametric study of planar artificial magnetic conductor surface," in *Proc. 23rd Nat. Radio Sci. Conf. (NRSC)*, Mar. 2006, pp. 1–8.

[118] P.-C. Tsai, "Design of compact mushroom structure with lumped elements to improve the performance of small antennas," M.S. thesis, Dept. Elect. Eng., Hsinchu, Taiwan, Aug. 2013.

[119] H. M. Al-Lawati, "Design and analysis of low profile circularly polarized antennas," Ph.D. dissertation, Dept. Electron. Elect. Eng., Univ. Sheffield, Sheffield, U.K., 2014.

[120] Y. Wang, J. Huang, and Z. Feng, "A novel fractal multi-band ebg structure and its application in multi-antennas," in *Proc. IEEE Antennas Propag. Soc. Int. Symp.*, Jun. 2007, vol. 136, no. 1, pp. 5447–5450.

[121] A. Aminian, F. Yang, and Y. Rahmat-Samii, "In-phase reflection and EM wave suppression characteristics of electromagnetic band gap ground planes," in *IEEE Antennas Propag. Soc. Int. Symp. Dig. USNC/CNC/URSI North Amer. Radio Sci. Meeting*, vol. 4, May 2004, pp. 430–433.

[122] L. Yang, M. Fan, F. Chen, J. She, and Z. Feng, "A novel compact electromagnetic-bandgap (EBG) structure and its applications for microwave circuits," *IEEE Trans. Microw. Theory Techn.*, vol. 53, no. 1, pp. 183–190, Jan. 2005.



**ADEL Y. I. ASHYAP** received the B.Eng., M.Eng., and Ph.D. degrees in electrical engineering from Universiti Tun Hussein Onn Malaysia (UTHM), Johor, Malaysia, in 2012, 2014, and 2019, respectively. He is currently a Postdoctoral Fellow of the Research Center of Applied Electromagnetics, Faculty of Electrical and Electronic Engineering, UTHM. He has authored or coauthored numbers of journals and proceedings. His research interests include electromagnetic bandgap (EBG), artificial magnetic conductor (AMC) for wireless body area networks (WBAN), microstrip antennas, and small antennas for biomedical devices. He has received the Chancellor Award for his final year project and a number of Gold, Silver, and Bronze medals in international and local competitions.



**SAMSUL HAIMI BIN DAHLAN** received the Ph.D. degree in signal processing and telecommunications from the Universite de Rennes 1, France, in 2012. He is supervising a numbers of bachelor's, master's, Ph.D. degree students and involved in several research projects sponsored by industry and government agencies. He has been a Senior Lecturer with the Faculty of Electric and Electronic Engineering, Universiti Tun Hussein Onn Malaysia (UTHM), since March 2012. He is currently a Principal Researcher with the Research Center for Applied Electromagnetics (EMCenter), UTHM, where has been as the Head, since April 2015. He has authored or coauthored a numbers of journals including the IEEE TRANSACTION ON ELECTROMAGNETIC COMPATIBILITY and the IEEE AWPL. His research interests include optical-microwave generators, focusing systems (dielectric lens and transmit array's synthesis), computational electromagnetic techniques, namely, and the BOR-FDTD and material characterizations.



**ZUHAIIRAH ZAINAL ABIDIN** received the Ph.D. degree from Bradford University, U.K., in 2011. She is currently a Principal Researcher with the Research Center for Applied Electromagnetics (EM Center), Universiti Tun Hussein Onn Malaysia. She has authored or coauthored a numbers of journals and proceedings, including the IEEE TRANSACTION ON ANTENNA AND PROPAGATION, IEEE ACCESS, and the IEEE AWPL. Her research interests include MIMO antennas, printed microstrip antennas, wearable antennas, electromagnetic bandgap (EBG) for wireless, and mobile and high-speed digital circuit applications.



**MUHAMMAD INAM ABBASI** received the B.Sc. degree in electrical engineering with major in telecommunication from the Centre for Advanced Studies in Engineering (CASE Islamabad), University of Engineering and Technology (UET), Taxilla, Pakistan, in 2008, and the master's and Ph.D. degrees in electrical engineering with Universiti Tun Hussein Onn Malaysia, in 2011 and 2016, respectively. He joined the Wireless and Radio Science Centre (WARAS), Universiti Tun Hussein Onn Malaysia (UTHM), as a Graduate Research Assistant, in 2009. He was a Postdoctoral Research Fellow of the Wireless Communication Centre (WCC), Universiti Teknologi Malaysia (UTM), in 2017 and 2018. He is currently a Senior Lecturer with the Faculty of Electrical and Electronic Engineering Technology, Universiti Teknikal Malaysia Melaka (UTeM). His recent research interests include high performance planar and printed antenna design, the study of passive and reconfigurable reflect array and planar reflector antennas, and investigation of novel materials for the design of enhanced performance antennas.



**MUHAMMAD RAMLEE KAMARUDIN** (Senior Member, IEEE) received the degree (Hons.) in electrical and telecommunication engineering from Universiti Teknologi Malaysia, Johor Bahru, Malaysia, in 2003, and the M.Sc. degree in communication engineering and the Ph.D. degree in electrical engineering from the University of Birmingham, Birmingham, U.K., in 2004 and 2007, respectively, under the supervision of Emeritus Professor Peter Hall. He has been an Associate Professor with the Faculty of Electrical and Electronic Engineering, Universiti Tun Hussein Onn Malaysia, since May 2019. Prior to this appointment, he was a Senior Lecturer with the Centre for Electronic Warfare, Information, and Cyber, Cranfield Defense and Security, Cranfield University, U.K., and an Associate Professor with the Wireless Communication Centre, Universiti Teknologi Malaysia. He holds a SCOPUS H-Index of 23 with over 2000 citations. He has authored a book chapter of a book entitled *Antennas and Propagation for Body-Centric Wireless Communications*. He has published over 240 technical articles in leading journals and international proceedings including the IEEE TRANSACTION ON ANTENNAS AND PROPAGATION, the IEEE ANTENNAS AND WIRELESS PROPAGATION LETTER, the *IEEE Antenna Magazine*, IEEE ACCESS, *International Journal of Antennas and Propagation*, *Progress in Electromagnetic Research, Microwave and Optical Technology Letters*, and *Electronics Letters*. His research interests include antenna design for 5G/6G, MIMO antennas, array antenna for beam-forming and beam steering, wireless on-body communications, in-body communications (implantable antenna), RF and microwave communication systems, and antenna diversity. He is a member of the IET, the IEEE Antennas and Propagation Society, the IEEE Communication Society, the IEEE Microwave Theory and Techniques Society, and the IEEE Electromagnetic Compatibility Society. He is an Executive Member of Antenna and Propagation of Malaysia Chapter. He is an Associate Editor of *Electronics Letters* and *IET Microwaves, Antennas, and Propagation*. He is also an Academic Editor of the *International Journal of Antennas and Propagation*.



**HUDA A. MAJID** received the B.Eng. degree (telecommunication) and the M.Eng. and Ph.D. degrees in electrical engineering from Universiti Teknologi Malaysia, from Universiti Teknologi Malaysia, in 2007, 2010, and 2013, respectively. He is currently a Lecturer with the Department of Electrical Engineering Technology, Faculty of Engineering Technology, Universiti Tun Hussein Onn Malaysia. He has published over 50 articles in journals and conference papers. His research interests include the design of microstrip antennas, small antennas, reconfigurable antennas, metamaterials structures, metamaterial antennas, and millimeter wave antennas.



**MUHAMMAD HASHIM DAHRI** received the B.E. degree in telecommunications from the Mehran University of Engineering and Technology (MUET), Pakistan, in 2010, the master's degree by research in electrical engineering from Universiti Tun Hussein Onn Malaysia (UTHM), in 2014, and the Ph.D. degree from the Wireless Communication Centre (WCC), Universiti Teknologi Malaysia (UTM), in 2019. He is currently a Postdoctoral Research Fellow of Universiti Tun Hussein Onn Malaysia (UTHM). He has authored over 25 research articles in various indexed journals and conference proceedings. His research interests include reflectarray antennas, planar printed antennas, and tunable materials for antenna design.



**MOHD HAIZAL JAMALUDDIN** received the bachelor's and master's degrees in electrical engineering from Universiti Teknologi Malaysia (UTM), Malaysia, in 2003 and 2006, respectively, and the Ph.D. degree in signal processing and telecommunications from the Université de Rennes 1, France, in 2009, with a focus on microwave communication systems and specially antennas such as dielectric resonator and reflectarray and dielectric dome antennas. He is currently an Associate Professor with the Wireless Communication Centre, School of Electrical Engineering, Universiti Teknologi Malaysia. He has published more than 100 articles in reputed indexed journals and conference proceedings. His research interests include dielectric resonator antennas, printed microstrip antennas, MIMO antennas, and DRA reflectarray antennas.



**AKRAM ALOMAINY** (Senior Member, IEEE) received the M.Eng. degree in communication engineering and the Ph.D. degree in electrical and electronics engineering (specialized in antennas and radio propagation) from the Queen Mary University of London (QMUL), London, U.K., in 2003 and 2007, respectively. In 2007, he joined the School of Electronic Engineering and Computer Science, QMUL, where he is currently an Associate Professor (Senior Lecturer) with the Antennas and Electromagnetics Research Group. He is a member of the Centre for Intelligent Sensing, Institute of Bioengineering, QMUL. He has authored or coauthored a book, five book chapters, and more than 220 technical articles (3900+ citations and H-index 29) in leading journals and peer-reviewed conferences. His current research interests include small and compact antennas for wireless body area networks, radio propagation characterisation and modelling, antenna interactions with human body, computational electromagnetic, advanced antenna enhancement techniques for mobile and personal wireless communications, and advanced algorithm for smart and intelligent antenna and cognitive radio systems. He is a member of the IET, a Fellow of the Higher Education Academy, U.K., and a College Member of the Engineering and Physical Sciences Research (EPSRC), U.K., and its ICT prioritisation panels. He was a recipient of the Isambard Brunel Kingdom Award, in 2011, for being an outstanding young science and engineering communicator. He was selected to deliver a TEDx talk about the science of electromagnetic and also participated in many public engagement initiatives and festivals. He is also a Reviewer of many funding agencies around the world including the Expert Swiss National Science Foundation Research, EPSRC, and the Medical Research Council, U.K. He was an Elected Member of the International Union of Radio Science (URSI), U.K., panel to represent the U.K. interests of URSI Commission B (from September 1, 2014 to August 31, 2017). He has managed to secure various research projects funded by research councils, charities, and industrial partners on projects ranging from fundamental electromagnetic to wearable technologies. He is the Leader of wearable creativity research with the QMUL. He has been invited to participate at the Wearable Technology Show, in 2015, Innovate U.K., in 2015, and in the recent wearable challenge organised by Innovate U.K. IC Tomorrow as a Leading Challenge Partner to support SMEs and industrial innovation.

• • •